Food & Function

ROYAL SOCIETY OF CHEMISTRY

PAPER

View Article Online
View Journal | View Issue

Cite this: *Food Funct.*, 2025, **16**, 1969

Tamarindus indica sub-products as potential tools for simultaneous management of diabetes and obesity†

Gustavo Henrique Souza,[a] Beatriz Paes Silva,[a] Gabriel Arcanjo Viana Neto,[a] Tiane C. Finimundy,[b,c] Thalita Faleiro Demito Santos,[a] Paulo Sergio Alves Bueno,[a] Felipe de Oliveira Souza,[d] Eduardo J. Pilau,[d] Lillian Barros,[b,c] Jurandir F. Comar,[a] Livia Bracht,[a] Rosane M. Peralta,[a] Adelar Bracht[a] and Anacharis B. Sá-Nakanishi*[a]

Aiming at valorizing industrial wastes of tamarind, the present work evaluated the actions of seed, leaf and peel extracts on starch and fat absorption through starch and triglyceride tolerance tests in mice. The actions of all extracts on the α-amylase and lipase were also characterized using classical kinetic assays. All extracts inhibited starch digestion *in vivo*, but the seed extract was the most effective one with an ID_{50} of 151.4 mg kg^{-1}. The mechanism behind this inhibition probably involves the pancreatic α-amylase, which was strongly inhibited by the seed extract under *in vitro* conditions (IC_{50} = 13.3 μg mL^{-1}) and much less strongly by the leaf and peel extracts (IC_{50} values in the vicinity of 400 μg mL^{-1}). The pancreatic lipase, conversely, was inhibited solely by the seed extract, with an IC_{50} of 31.5 μg mL^{-1}. As a consequence of this property, the seed extract also inhibited triglyceride absorption, as indicated by olive oil tolerance tests, which revealed an ID_{50} of 214.9 mg kg^{-1}. The seed extract also possessed the strongest antioxidant capacity and the highest content in phenolic groups. Chemical analyses revealed that all extracts present a great variety of phenolic compounds and that the seed extract possesses at least 5 unique compounds (ursodiol, masoprocol, lenticin, chenodeoxycolic acid and 13-keto-9*Z*,11*E*-octadecadienoic acid), which, according to docking studies, could be involved in the inhibition of both α-amylase and lipase. The overall conclusion is that the tamarind seed extract displays great potential for being used in the management of obesity and diabetes.

Received 18th September 2024,
Accepted 13th January 2025

DOI: 10.1039/d4fo04536j

rsc.li/food-function

1. Introduction

Obesity is a metabolic disorder characterized by the abnormal or excessive accumulation of body fat, which is associated with various comorbidities, including dyslipidemia, diabetes, fatty liver, atherosclerosis, hypertension, and cardiovascular disease.[1] The World Health Organization classifies obesity as a pandemic disease, which is affecting an increasing number of people annually.[1] One of the therapeutic approaches for the treatment and management of this disease involves inhibiting the α-amylase and lipase enzymes,[2] which play crucial roles in carbohydrate and fat digestion and their absorption by the gut cells.[3,4] Although anti-obesity drugs are available on the market, a lot of adverse effects are related to them, which leads to the discontinuation of therapy by the patients.[5] For this reason, natural compounds have been investigated as safe alternatives in the treatment of obesity. Polyphenols, found in several natural sources, can inhibit digestive enzymes, reducing food absorption and lengthening the digestive process, which may facilitate weight loss and offer significant health benefits.[6]

Tamarindus indica is a species of the *Leguminosae* family and *Caesalpiniaceae* subfamily, native to the African savannah and found in many tropical and subtropical countries. The fruit, known as tamarind, is a slightly curved pod, which can be structurally separated into four parts:brittle shell, rusty-

[a]*Hepatic Metabolism Lab, Department of Biochemistry, State University of Maringá, Maringá, PR, Brazil. E-mail: absnakanishi@uem.br, gustavo.hsouza99@gmail.com, paessilvabeatriz@gmail.com, pg405519@uem.br, tsantos@prof.unipar.br, lbracht@uem.br, psabueno2@uem.br, rmperalta@uem.br, jfxomar@uem.br, abracht@uem.br; Tel: +55 44 30114711 or 55 44 999026769*
[b]*Centro de Investigação de Montanha (CIMO), Instituto Politécnico de Bragança, Campus de Santa Apolónia, 5300-253 Bragança, Portugal. E-mail: tiane@ipb.pt, lillian@ipb.pt*
[c]*Laboratório Associado para a Sustentabilidade e Tecnologia em Regiões de Montanha (SusTEC), Instituto Politécnico de Bragança, Campus de Santa Apolónia, 5300-253 Bragança, Portugal*
[d]*Department of Chemistry, State University of Maringá, Maringá, PR, Brazil. E-mail: oliveirasouza.felipe@gmail.com, ejpilau@uem.br*

† Electronic supplementary information (ESI) available. See DOI: https://doi.org/10.1039/d4fo04536j

brown skin, edible acidic-sweet pulp, and oval shiny brown seeds.[7] According to the World Health Organization, tamarind fruit and seed are sources of amino acids (82%) except tryptophan.[8] The pulp is widely used for both domestic and industrial purposes, including culinary preparations, like curries, chutneys, sauces, ice creams, and beverages.[9]

Various parts of the plant have been studied and used by the population for medicinal purposes, thanks to its rich nutritional value which results in economic importance.[9] Tamarind leaves are used in Indonesian folk medicine to treat hyperlipidemia.[10] Actually, numerous studies have revealed that *T. indica* exerts glucose and lipid-lowering activities and that it may be used to treat obesity and diabetes. *Tamarindus indica* pulp extract (50 to 500 mg kg^{-1}) decreased the levels of total plasma cholesterol, low-density lipoprotein, triglycerides and glucose, and increased HDL, with the concomitant reduction of body weight in obese, hypercholesterolemic and diabetic animals.[11–14] There are also reports about the weight-reducing and hypolipidemic activities of the pulp extract of *T. indica* (2.7 to 4.5 g kg^{-1}) when administered for 28 days to healthy rats fed with a standard diet.[15]

The inclusion of tamarind seeds in the diet (4% and 8%) lowered the cholesterol levels of normal rats and suppressed the high blood glucose levels of hyperglycemic rats.[16] Administration of a seed extract (1.2 g kg^{-1}), in addition to inducing substantial diminution in the levels of glucose, total cholesterol and triacylglycerols in blood, also normalized the glycogen levels and glucose 6-phosphatase activity in the liver of diabetic rats.[17] The tamarind leaf extract was also effective in reducing hyperlipidemia and in reducing glucose levels in rats.[18] Some of the effects were explained by the capacity of the extracts to sensitize the insulin receptor, inhibit the fatty acid synthase (FAS), reduce the plasma leptin content, stimulate SRBP-1c mRNA expression and enhance the efficiency of the antioxidant defense system.[11,17,19,20]

Some publications infer that the clinical changes mentioned above result from α-amylase and lipase inhibition by *Tamarindus indica.*[2] Buchholz and Melzig (2016)[21] reported that the peel methanolic extract of *Tamarindus indica* showed a high anti-lipase activity (IC_{50}: 152.0 ± 7.0 μg mL^{-1}) and the aqueous extract showed a high anti-amylase (IC_{50}: 139.4 ± 9.0 μg mL^{-1}) activity. On the other hand, Bhutkar and Bhise (2012)[22] displayed weak inhibitions by leaf, seed and peel extracts, since a concentration of 9 mg mL^{-1} was needed to achieve an inhibition of about 70%. *In vivo* assays showed that a *T. indica* seed powder (1.25 g kg^{-1}) inhibited glucose absorption by the gut cells of rats.[23]

The observations that were summarized above strongly indicate that tamarind affects lipid and carbohydrate metabolism. Another great possibility is an action on triglyceride and starch absorption from the intestinal tract. However, the inhibitions of both α-amylase and lipase have not yet been entirely clarified in terms of their kinetic mechanisms and potencies nor is it entirely clear what doses are required *in vivo* or even if they occur in animals. It is important to note that the food industries discard a high quantity of tamarind sub-products (leaves, seeds and peels) every year, and they are widely accepted as cheap sources of raw materials for various industrial purposes. Recent research has emphasized their potential for being repurposed into functional foods and therapeutic products, showcasing their cost-effectiveness and innovative applications in treating metabolic disorders.[10–15] Preparations obtained from these by-products are abundant in bioactive compounds and exhibit various mechanisms of action, making them particularly valuable in addressing the underlying causes of diabetes and obesity.[24] This approach represents a promising strategy to improve treatment effectiveness and patient adherence, since there is no single definitive treatment available and the existing pharmacotherapy requires the continuous use of numerous drugs. Moreover, repurposing tamarind by-products aligns with sustainable development goals and contributes to advancing circular bioeconomy. By transforming food industry by-products into high-value preparations, these efforts have the potential of delivering significant public health benefits while fostering environmental sustainability.

Therefore, in order to integrate tamarind sub-products into the productive chain and to establish a sustainable alternative for them, the present study aimed at evaluating and comparing the effects of tamarind seeds, leaves and peels on α-amylase and lipase activities both *in vitro* and *in vivo* in the hope of identifying a preparation that could work as an alternative or complementary medicine in the treatment and management of diabetes and obesity.

2. Materials and methods

2.1. Chemicals

Porcine pancreatic α-amylase (type IV-B), porcine pancreatic lipase (typo II), potato starch, 2,2-azinobis(3-ethylbenzothiazoline-6-sulphonic acid) (ABTS), 6-hydroxy-2,5,7,8-tetramethylchromane-2-carboxylic acid (Trolox), 2,2-diphenyl-1-picrylhydrazyl (DPPH), 2,20-azobis(2-amidinopropane) dihydrochloride (AAPH), and Tris were purchased from Sigma-Aldrich Co. (St Louis, MO, USA). Excipient-free acarbose and orlistat were obtained from Manipulação Farmácia São Paulo (Maringá). All chemicals were of the highest possible degree of purity.

2.2. Animals

Male Swiss mice weighing 30 and 40 g were used in all experiments. The animals were fed *ad libidum* with a standard laboratory diet (Nuvilab, Colombo, Brazil) and maintained under a regular light–dark cycle. For all experiments *in vivo*, the mice were starved for 18 h before the experiments. The Ethics Committee previously approved all experiments of animal experimentation at the University of Maringá (protocol number 9905181121).

2.3. Preparation of hydroethanolic extracts of *T. indica*

The tamarind fruit and leaves were collected from a rural property in Marialva city, Brazil. Different parts of the plant, namely leaves, seeds and peels, were separated, dried in a

recirculation oven at 45 °C and ground to a fine powder. The powder of each part was weighed and suspended in a 70% hydroalcoholic solution (10 g per 100 mL), kept on a rotary shaker (120 rpm) for 2 hours and subjected to filtration using a vacuum pump. The solid residue was subjected to two additional and successive extractions. The filtrate was maintained in an oven at 45 °C for ethanol total evaporation. The solution was lyophilized and stored at −20 °C in an amber bottle.

2.4. Evaluation of *in vitro* antioxidant activity and total phenolic assay

Three different chemical methods were used to evaluate the antioxidant activity: reduction power of the ferric ion (FRAP), reduction of the 2,2-diphenyl-1-picrylhydrazyl radical (DPPH), and reduction of the 2,2-azinobis(3-ethylbenzothiazoline-6-sulphonate) cation ($ABTS^{+}$). Successive dilutions of the various extracts were made and used for assaying the antioxidant activity of the samples. DPPH, ABTS and FRAP assays were conducted as described previously.[25] The percentage of DPPH and ABTS discoloration was calculated using the following equation: $[(Abs_{control} - Abs_{sample})/Abs_{control}] \times 100$, and was expressed as IC_{50} values (sample concentration, μg mL^{-1}, providing 50% of maximum antioxidant activity). FRAP was expressed as k_{FRAP}, which corresponds to the initial slope of the line obtained from absorbance *versus* extract concentration curves, expressed as min^{-1}.[26]

Total phenolic contents in extracts were determined by using the Folin–Ciocalteu reagent and expressed as gallic acid equivalents per mg extract.[27]

2.5. Pancreatic α-amylase assay and kinetics

The activity of the porcine α-amylase was determined as the rate of reducing sugar formation from starch, which was utilized as the substrate of the reaction.[28–30] The reaction was run in a buffered medium (20 mM phosphate buffer, 6.7 mM NaCl, pH 6.9) in the presence and absence of the inhibitor (tamarind peel, seed, or leaf extracts). The final concentration of starch was between 0.05 and 1 g per 100 mL and the extract concentrations were in the range between 1 and 500 μg per mL. The α-amylase concentration in all assays was 0.75 units per mL. The enzyme solutions plus inhibitors were incubated at 37 °C for 10 minutes before starting the reaction by adding the substrate solution. The reaction was started by the addition of starch. After 10 minutes, the reaction was stopped in boiling water for 5 minutes. The reducing sugar content was determined by the 3,5-dinitrosalicylate method.[30] The absorbance, which is directly proportional to the concentration of reducing sugar, was determined at 540 nm. The reaction rates were expressed as μmol per minute.

2.6. Pancreatic lipase assay and kinetics

The activity of the pancreatic lipase was determined using *p*-nitrophenyl-palmitate as the substrate, which was suspended in isopropanol and sonicated until complete solubilization.[31] The porcine pancreatic lipase was suspended in Tris-HCl buffer at concentrations of 600 U mL^{-1} and centrifuged (2000*g*, 5 min) and the supernatant was utilized in the assay. The reaction medium was 10 mM Tris-HCl buffer (pH 8.2) containing *p*-nitrophenyl-palmitate at various concentrations in the range up to 600 μM, according to the experimental protocol. The *T. indica* extracts (seed, peel and leaf) were added for final concentrations up to 250 μg mL^{-1}. After 5 minutes at 37 °C, the reaction was started by adding 0.1 mL of the enzyme solution and kept for 10 minutes. The reaction was stopped by dipping the tubes in boiling water for 5 minutes. After that, the solution was centrifuged (21 000*g* for 10 min) and the concentration of *p*-nitrophenol was measured at 410 nm. The reaction rates were expressed as μmol per minute using an extinction coefficient of 1.83×10^4 M^{-1} cm^{-1}.

2.7. Oral starch and glucose tolerance tests in mice

Fasted animals (18 hours) were used for these experiments. The number of animals in each group was between 3 and 8. The number of animals in each group was established based on the previous experience of the research group and adherence to the principle of minimizing the use of animals.[28,29,31] No animals were excluded from the study. The administration route was intragastric (by gavage). Control groups received commercial corn starch (1 g per kg) and the negative controls received filtered water.[28] *T. indica* extracts were administered in doses of 100, 250 and 500 mg per kg of body weight to different groups of mice, followed by the administration of commercial corn starch. Another group was treated with acarbose at a dose of 50 mg kg^{-1} (reference substance) and commercial corn starch. Plasma glucose was determined at time periods of 0, 30, 60, 90 and 120 minutes after corn starch administration. Blood samples were collected from the tail vein and analyzed using a glucometer (AccuChek®). The glucose tolerance test was performed as described above, except that glucose (1.5 g per kg) was given to the animals in place of starch.

2.8. Oral triglyceride tolerance tests in mice

Intestinal triglyceride absorption was determined by means of the tolerance test to olive oil after 18 hours of fasting.[32] The number of animals in each group was between 3 and 6. The number of animals in each group was determined based on the previous experience of the research group.[27,28,30] *T. indica* extracts were solubilized in filtered water and administered intragastrically at doses of 250 and 500 mg per kg of body weight to different groups of animals. The control group received just drinking water. The reference drug orlistat was given to another group (50 mg per kg). After drug or extract administration, all animals received olive oil (5 mL per kg) intragastrically. Plasma triglyceride levels were determined in blood samples collected from the tail vein at 0, 90, 180, 240 and 360 minutes after olive oil administration. The measurement of blood triglycerides was done using an Accutrend® Plus Roche triglyceride meter, which is an end-point enzymatic-colorimetric assay that quantifies the glycerol moiety of the triglycerides.

2.9. Analysis of flavonoids, phenolic acids and tannins

Lyophilizates of the leaf, peel and seed extracts were re-dissolved in water and analyzed by high-performance liquid chromatography with photodiode array detection–electrospray ionization multiple-stage mass spectrometry (HPLC-DAD-ESI/MSn) (Dionex Ultimate 3000 UPLC, Thermo Scientific, San Jose, CA, USA).[31,33] For the double online detection, 280 and 370 nm were used as the preferred wavelengths for DAD. The mass spectrometer (MS) was connected to the HPLC system *via* the DAD cell outlet. The MS detection was performed in the negative mode, using a Linear Ion Trap LTQ XL mass spectrometer (Thermo Finnigan, San Jose, CA, USA) equipped with an ESI source. The identification of the compounds was performed using standard compounds, when available, by comparison of their retention times and UV–vis and mass spectra, and also by comparing the obtained information with the data available in the literature, giving a tentative identification. For quantitative analysis, a calibration curve for each available standard was constructed based on the UV signal. For the identified compounds for which a commercial standard was not available, the quantification was performed using the calibration curve of the most similar available standard. The results were expressed as mg per gram extract.

2.10. Qualitative chemical analysis of the hydroethanolic extracts

To gain an insight into the extract's compositions beyond the flavonoids, phenolic acids and tannins, qualitative chromatographic analyses coupled with fragmentation procedures were performed. The Global Natural Product Social Molecular Networking (GNPS) platform was used for aiding identification and posterior annotation. For the procedure, samples of seed, leaf and peel extracts were solubilized in 500 μL of water/acetonitrile (1 : 1; v : v), separated by ultra-high-performance liquid chromatography (UPLC) and automatically analyzed by electrospray ionization tandem mass spectrometry (UHPLC-ESI-MS/MS; Nexera X2, Shimadzu, Japan) and impact II mass spectrometry (quadrupole time-of-flight geometry; Bruker Daltonics Corporation, Germany).

The ultra-high-performance liquid chromatograph was equipped with a UPLC CSH C18 column (Acquity, Waters, USA, 1.7 μm, 2.1 × 100 mm) under a flow rate of 0.2 mL min^{-1}. Elution was performed using a gradient mixture of solvents A (H_2O with 0.1% formic acid, v : v) and B (acetonitrile with 0.1% formic acid, v : v) under the following conditions: 2% B at 0–1 min, 30% B at 1–3 min, 80% B at 3–20 min, 98% B at 20–32 min, and maintained at 2% B at 32–38 min at 40 °C. The instrument was calibrated using a sodium formate solution (10 mmol L^{-1} isopropanol : water; 1 : 1; v : v). The ionization source in the mass spectrometer was operated in the positive ((+)-ESI) and negative ((−)-ESI) ionization modes, set at 3500 V, with a final plate potential of −500 V. Dry gas parameters were set to 8 L min^{-1} at 200 °C, with a nebulization gas pressure of 4 bar. Data were acquired in the *m*/*z* range of 50–2000 at an acquisition rate of 7 Hz. The ions were selected for automatic fragmentation (AutoMS/MS). Data collection and processing were performed using Hystar Application version 3.2 and Otof Control software (Bruker Daltonics Corporation).

The molecular networking data were exported to Cytoscape 3.7.1 software[34] for visualization. Product ion spectra with resemblances to those in the mass spectral libraries were manually verified, and the mass error was calculated, using a mass error tolerance of less than 10 ppm. These annotations are regarded as tentative annotations based on spectral library similarity or characterized compound class based on spectral similarity to known compounds of a chemical class.[35]

2.11. Molecular docking

Molecular docking was performed with the purpose of identifying the molecules in the seed extracts with the highest probability of acting as inhibitors of pancreatic α-amylase and lipase. Data on the structures of 19 molecules from the seed extract, identified by UHPLC-ESI-MS/MS, were obtained from the PubChem database (**https://pubchem.ncbi.nlm.nih.gov/**) and constructed using Open Babel.[36] The 3D structures of enzymes were acquired from the Protein Data Bank (rcsb.org). The α-amylase from *Homo sapiens* (E.C.: 3.2.1.1, PDBid: 1XD0, 2 Å resolution),[37] co-crystallized with the inhibitor acarbose (ARE), a Ca^{2+} ion for the protein stabilization and four structural water molecules (536, 546, 588, and 766), essential for interaction with ARE, were used (Fig. S1†). The lipase from *Homo sapiens* (EC 3.1.1.3, PDB ID: 1LPB, resolution: 2.46 Å), bound to methoxyundecylphosphinic acid (MUP), a synthetic inhibitor, as well as the cofactors Ca^{2+} and colipase (Fig. S2†) was performed.[38] The stereochemistry of both enzymes was assessed using Ramachandran plots (Fig. S1A and S1B†).[39] The enzyme–ligand complexes underwent energy minimization cycles using the NAMD2/VMD software packages.[40,41] In this step, each complex was solvated with TIP3P water, and Na^+ and Cl^- counterions were added to neutralize the system. Energy minimization occurred in two cycles for each complex. In the first cycle, the co-crystallized ligands were kept fixed in space, while the protein chain, salts and solvent were minimized for 30 000 conjugate gradient steps. In the second cycle, only the ligands were free to move until energy minimization was reached. The final structures from these simulations were used for the molecular virtual screening.

Docking protocols were validated through the redocking of the inhibitors mentioned for each enzyme using three distinct programs: AutoDock Vina,[42] AutoDock 4.2.3,[43] implemented in the PyRx 0.8 graphical interface,[44] and GOLD-v5.4.0.[45] For AutoDock Vina[42] and AutoDock 4.2.3, standard search and scoring algorithms were applied, with a grid spacing of 0.375 Å, in box dimensions of 25 Å × 25 Å × 25 Å and 50 Å × 50 Å × 50 Å, respectively. For the GOLD program, the search algorithm used was GA, and the scoring function CHEMPLP with ChemScore and GoldScore with ASP for lipase and amylase, respectively, in a sphere with a radius of 25 Å centered on the inhibitor. After re-docking, the AutoDock Vina and GOLD programs were used for docking studies with α-amylase, while AutoDock 4.2.3 and GOLD were applied for lipase. The library of 19 tamarind seed extract molecules pre-

pared earlier was subjected to four simulations within each program. The molecular docking outcomes underwent assessment based on the parameters of binding architecture, binding energy, and potential interactions between the ligand and crucial protein residues.[46]

To filter and rank the best molecules docked to the enzymes, the mean relative score (MRS) was calculated considering the best scores from two different programs for each enzyme in accordance with eqn (1):[47]

$$\mathrm{MRS} = \frac{1}{N_\mathrm{p}}\left(\frac{S_{\mathrm{p}_1}}{\mathrm{BS}_{\mathrm{p}_1}} + \frac{S_{\mathrm{p}_2}}{\mathrm{BS}_{\mathrm{p}_2}} + \ldots\right); \quad (1)$$

N_p – the number of molecular docking programs used in the simulations, S_{p_1}, S_{p_2}, ... – the score of each ligand in the program, and $\mathrm{BS}_{\mathrm{p}_1}$, $\mathrm{BS}_{\mathrm{p}_2}$, ... – the corresponding best score obtained in each program among all ligands.

2.12. Least-squares fits, statistical criteria and data analyses

Numerical interpolation for the determination of the half-maximal inhibitor concentrations (EC_{50}) was done using Scientist software from MicroMath Scientific Software (Salt Lake City, UT). The same program was used for fitting the rate equations to the experimental initial rates of enzymatic activity by means of an iterative non-linear least-squares procedure. The decision about the most adequate model (equation) was based on the model selection criterion (MSC) and the standard deviations of the optimized parameters. The model selection criterion, which corresponds to the normalized Akaike Information Criterion, is defined as:[48]

$$\mathrm{MSC} = \ln\left[\frac{\sum_{i=1}^{n} w_i\left(Y_{\mathrm{obs}_i} - \bar{Y}_\mathrm{obs}\right)^2}{\sum_{i=1}^{n} w_i\left(Y_{\mathrm{obs}_i} - Y_{\mathrm{cal}_i}\right)^2}\right] - \frac{2p}{n}; \quad (2)$$

Y_obs are the experimental reaction rates, $\bar{Y}_\mathrm{obs}$ – the mean experimental reaction rate, Y_cal is the theoretically calculated reaction rate, w is the weight of each experimental point, n is the number of observations and p is the number of parameters of the set of equations. The model with the largest MSC value was considered the most appropriate, provided that the estimated parameters were positive. When the MSC values differed by less than 5%, the mode yielding the smallest standard deviations for the estimated parameters was considered the most appropriate one.

Statistical analysis was performed using GraphPad Prism software (version 8.0). The experimental data were expressed as the mean ± medium standard error and were analyzed using one-way analysis of variance (one-way ANOVA). Significant differences were determined by the Tukey *post-hoc* test. Differences were considered significant at $p \leq 0.05$.

3. Results and discussion

3.1. Antioxidant activity and total phenolic contents of the *T. indica* extracts

The yields of the hydroethanolic seed, leaf and peel extracts were 20, 16, and 11%, respectively. As a first step in the characterization of these extracts, *in vitro* antioxidant activities were determined. The results are shown in Table 1. The antioxidant capacities in the ABTS and DPPH assays were expressed in terms of the concentrations that scavenge 50% of both radicals (IC_{50}) during the incubation time (see Materials and methods). In both assays, the seed extract presented a higher antioxidant capacity in comparison with the other extracts, as reflected by the smaller IC_{50} values. Actually, the antioxidant activity of the seed extract was at least three times greater than that of the leaf and peel extracts. The antioxidant capacity of the extracts was additionally evaluated by measuring their capacity to reduce ferric ions. These experiments revealed that the seed extract has a higher capacity for reducing ferric ions (five times) than the leaf and peel extracts, as revealed by the rate constant k_frap.

Since the antioxidant capacity of plant extracts is frequently associated with phenolic groups, attempts were made to determine the total phenolic group content of each extract using the traditional Folin–Ciocalteu method.[49] The results are displayed in Table 1. They reveal that the total phenolic group content of the seed extract exceeds those of the leaf and peel extracts by factors of 2.3 and 2.0, respectively. In principle, this is consistent with the antioxidant activity of the extracts, which was also higher in the seed extract when compared to the other two extracts. The nature of these phenolic groups may encompass several types of compounds. Flavonoids, phenolic acids and tannins, for example, are likely candidates. However, it is well known that the Folin–Ciocalteu method for phenolic group determination is not specific as it reacts not only with flavonoids, phenolic acids and tannins,[49,50] but also with amino acids and carboxylic acids, for example.[49] Determination of the true participation of each class of com-

Table 1 Antioxidant activity and total phenolic group contents of the *T. indica* seed, leaf and peel extracts. Data are presented as mean ± mean standard errors (n = 3)

Parameter	Seed	Leaf	Peel
ABTS (IC_{50}) (μg mL^{-1})	6.21 ± 0.04^{a}	21.01 ± 1.04^{b}	34.05 ± 0.9^{c}
DPPH (IC_{50}) (μg mL^{-1})	4.69 ± 0.11^{a}	15.81 ± 1.11^{b}	18.40 ± 1.05^{b}
FRAP (k_frap) (min^{-1})	0.25 ± 0.08^{a}	0.045 ± 0.00^{b}	0.048 ± 0.003^{b}
Total phenolic groups (mg(GAE) g^{-1})	263.2 ± 4.30^{a}	130.9 ± 10.5^{b}	115.3 ± 6.20^{b}

GAE means gallic acid equivalents. Different superscript letters in the same line depict significant results in accordance with one-way ANOVA and Tukey's *post hoc* test ($p < 0.05$).

pounds, thus, requires specific identification and quantification of the main components of each extract.

3.2. Effects of the *T. indica* extracts on α-amylase and kinetics

The possible action of the tamarind extracts on the pancreatic α-amylase was investigated based on reports that preparations rich in phenolics are inhibitory to this enzyme. In the first experiments, the porcine pancreatic α-amylase was tested at various concentrations of each extract and with a fixed starch concentration, as described in the Materials and methods section. The results of these evaluations are shown together in Fig. 1. To facilitate interpretation by single inspection, the rates were expressed as fractions of each corresponding control (no extract present). Fig. 1 reveals that all extracts were inhibitory, but that the seed extract was much more effective. Inhibition occurred in a concentration-dependent manner and approximately 50% inhibition was achieved with peel and leaf extracts at concentrations close to 500 μg mL^{-1}. With the seed extract, however, inhibition was almost complete at the concentration of 100 μg mL^{-1} and numerical interpolation predicts 50% inhibition at the concentration of 13.3 μg mL^{-1}.

For improving the analysis of the α-amylase inhibition, the experiments in Fig. 1 were complemented further by measuring the reaction rates in the presence of varying substrate concentrations at various inhibitor concentrations. The results that were obtained with the seed extract are shown in Fig. 2. Panel A reproduces the experimental results, now expressed as absolute rates (v), obtained with a fixed substrate concentration ([S]) and varying extract concentrations ([I]), whereas panel B shows the results obtained at various fixed extract concentrations and varying substrate concentrations. The v *versus* [S] relationships are typical saturation curves, progressively depressed upon each increase in the fixed extract (inhibitor) concentration, with no signs of convergence at high substrate

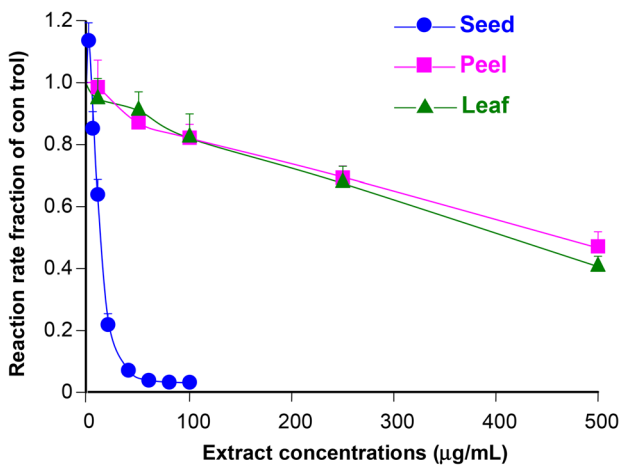

Fig. 1 Concentration dependences of the porcine pancreatic α-amylase activity on the concentration of *T. indica* seed, peel and leaf extracts. Initial reaction rates were measured as described in the Materials and methods section and are represented as fractions of the corresponding controls (no extract present) against the extract concentrations. Each datum point is the mean ± MSE of four determinations.

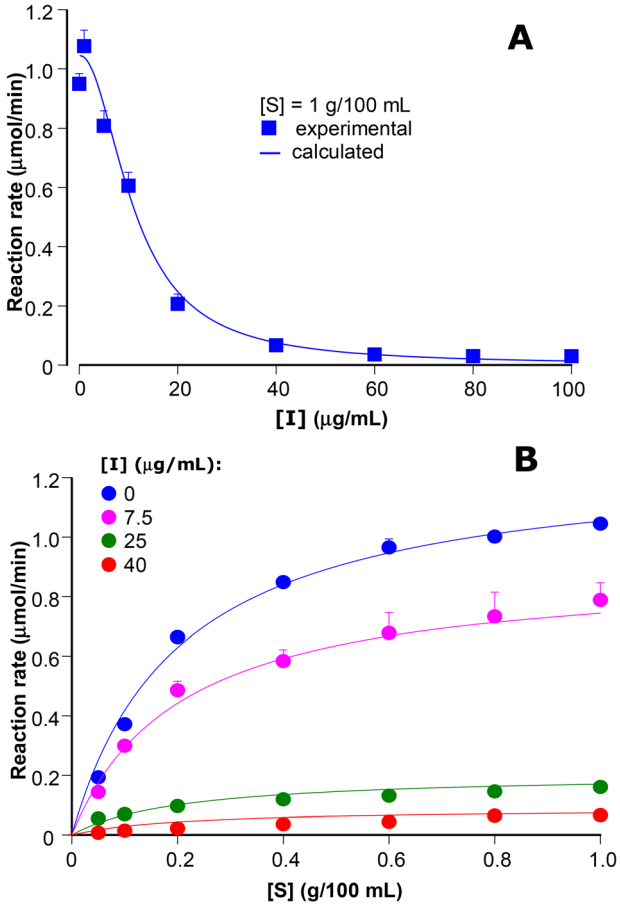

Fig. 2 Reaction rates of the porcine pancreatic α-amylase obtained by varying simultaneously the concentrations of the *T. indica* seed extract ([I]) and the substrate ([S]; starch). (A) Effect concentration dependence; (B) kinect analysis. Each datum point is the mean of four determinations. The lines running through the experimental points were calculated using the optimized parameters obtained by fitting eqn (1) to the experimental data by means of a nonlinear least-squares procedure. The optimized parameters were: K_M, 0.205 ± 0.018 g per 100 mL; V_{max} = 1.254 ± 0.031 μmol min^{-1}; $\bar{K}_{i1}$ = 10.944 ± 1.846 μg mL^{-1}; $\bar{K}_{i2}$ = 11.051 ± 0.681 μg mL^{-1}. Goodness of fit indicators: sum of squared deviations, 0.0337; MSC, 4.867; correlation, 0.997.

concentrations. This feature does not suggest competitive inhibition, but rather non-competitive or mixed inhibition. An answer to this question was obtained by fitting several models using a non-linear least-squares procedure and applying the statistical criteria outlined in the Materials and methods section for deciding about the best model (kinetic mechanism). These calculations revealed that the best model is the one described by the following equation:

$$v = \frac{V_{max}[S]}{K_M\left(1 + \frac{[I]^2}{(\bar{K}_{i1})^2}\right) + [S]\left(1 + \frac{[I]^2}{(\bar{K}_{i2})^2}\right)}. \quad (3)$$

In eqn (3), K_M and V_{max} represent the Michaelis constant and the maximal reaction rate, respectively. The inhibition constants are $\bar{K}_{i1}$ and $\bar{K}_{i2}$, actually composite inhibition constants, as

denoted by the overline. Eqn (3) describes mixed or non-competitive inhibition, but the quadratic terms in the denominator denote parabolic inhibition. Parabolic inhibition occurs when the enzyme binds simultaneously to at least two inhibitors at one or two sites. In this specific case, eqn (3) reveals that the complexes EI_2 and SEI_2 are probably the most common inhibitory complexes in the presence of the seed extract. Values of the optimized parameters are listed in the legend of Fig. 2 in addition to the statistical indicators. It should be remarked that eqn (3) was fitted simultaneously to both the *v versus* [I] and the *v versus* [S] curves. It can be seen that the values of $\bar{K}_{i1}$ and $\bar{K}_{i2}$ are very close to each other, an indication of simple non-competitive inhibition rather than mixed inhibition. They are also very close to the IC_{50} value determined above, an expected outcome for non-competitive inhibition, in which the IC_{50} is independent of the substrate concentration. Fig. 2 also allows the comparison of the experimental and calculated curves. The latter was obtained by introducing the optimized parameters into eqn (3). Inspection reveals that theory and experiment agree fairly well, without systematic deviations. This is valid also for the relation between the reaction rate and the inhibitor concentration, which is shown in panel A.

The kinetics of the inhibitions caused by the peel and leaf extracts were investigated in the same way as described above for the seed extract. Fig. 3 shows the results of the kinetic analysis of the peel extract data. In this case, the best fit to the experimental data was given by using eqn (4):

$$v = \frac{V_{max}[S]}{K_M\left(1+\frac{[I]}{(K_{i1})}\right)+[S]\left(1+\frac{[I]}{(K_{i2})}\right)}. \quad (4)$$

This equation is similar to eqn (3), but there are no quadratic [I] terms in the denominator. It describes, thus, linear mixed or non-competitive inhibition in which the EI and ESI complexes are formed. The optimized values of the kinetic parameters are given in the legend to Fig. 3. K_{i1} and K_{i2} are different, K_{i2} being somewhat smaller than K_{i1}, though the difference is not very pronounced, and the standard errors are relatively high. Even so, it is appropriate to conclude that the complex ESI is more readily formed than the EI complex, what characterizes mixed inhibition. Agreement between theory and experiment can be considered good as the theoretical lines calculated employing eqn (4) and using the optimized parameters cover with great approximation the experimental points. This is true here again for both the *v versus* [I] as well as the *v versus* [S] relationships.

Fig. 4 shows the outcomes of the kinetic analysis of the leaf extract data. The equation that gave the best fit was the following:

$$v = \frac{V_{max}[S]}{K_M+[S]\left(1+\frac{[I]}{K_{i2}}\right)}. \quad (5)$$

Eqn (5) describes uncompetitive inhibition, a mechanism in which the inhibitor binds solely to the ES complex, forming, thus, the ESI complex. Nevertheless, Fig. 4 reveals that agreement between theory and experiment is not as good as it was with the results obtained with the seed and peel extracts (compared with

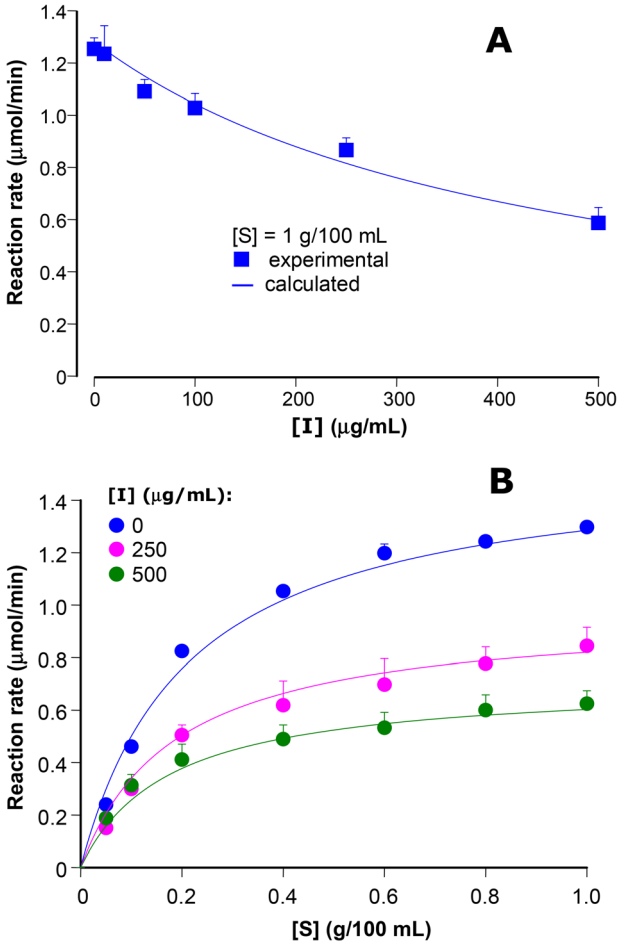

Fig. 3 Reaction rates of the porcine pancreatic α-amylase obtained by varying simultaneously the concentrations of the *T. indica* peel extract ([I]) and the substrate ([S]; starch). (A) Effect concentration dependence; (B) kinect analysis. Each datum point is the mean of four determinations. The lines running through the experimental points were calculated using the optimized parameters obtained by fitting eqn (3) to the experimental data by means of a nonlinear least-squares procedure. The optimized parameters were: K_M, 0.210 ± 0.019 g per 100 mL; V_{max} = 1.556 ± 0.039 μmol min^{-1}; K_{i1} = 603.08 ± 0.198 μg mL^{-1}; K_{i2} = 417.19 ± 40.28 μg mL^{-1}. Goodness of fit indicators: sum of squared deviations, 0.0364; MSC, 4.599; correlation, 0.996.

Fig. 2 and 3). The most evident deviation between theory and experiment is that one in the *v versus* [I] curve, in which a systematic deviation at the highest extract concentration is apparent. Furthermore, the data in the *v versus* [S] curves present considerable dispersion. Anyway, the value of the inhibition constant is relatively high (see the legend to Fig. 4), comparable to those found with the peel extract and much higher than those obtained in the analysis of the seed extract data. Clearly, the kinetic analyses confirm that the seed extract is by far a better inhibitor of the α-amylase than the peel and leaf extracts.

3.3. Effects of the tamarind seed extract on the pancreatic lipase activity and kinetics

Considering that there is previous evidence that a tamarind preparation inhibits pancreatic lipase,[21] the activity of this

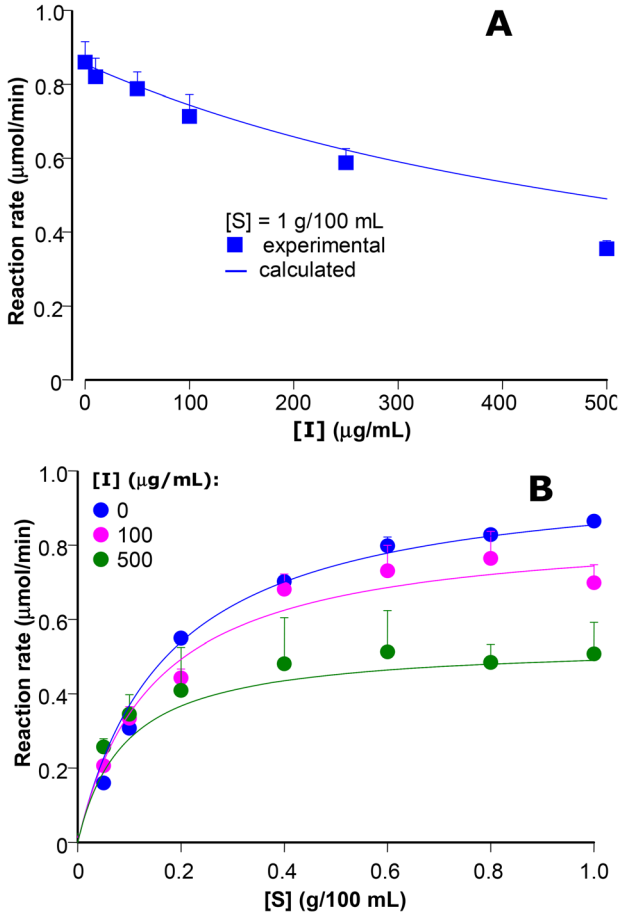

Fig. 4 Reaction rates of the porcine pancreatic α-amylase obtained by varying simultaneously the concentrations of the *T. indica* leaf extract ([I]) and the substrate ([S]; starch). (A) Effect concentration dependence; (B) kinect analysis. Each datum point is the mean of four determinations. The lines running through the experimental points were calculated using the optimized parameters obtained by fitting eqn (4) to the experimental data by means of a nonlinear least-squares procedure. The optimized parameters were: K_M, 0.172 ± 0.021 g per 100 mL; V_{max} = 1.001 ± 0.0338 μmol min^{-1}; K_{i2} = 573.46 ± 66.47 μg mL^{-1}. Goodness of fit indicators: sum of squared deviations, 0.0581; MSC, 3.347; correlation, 0.985.

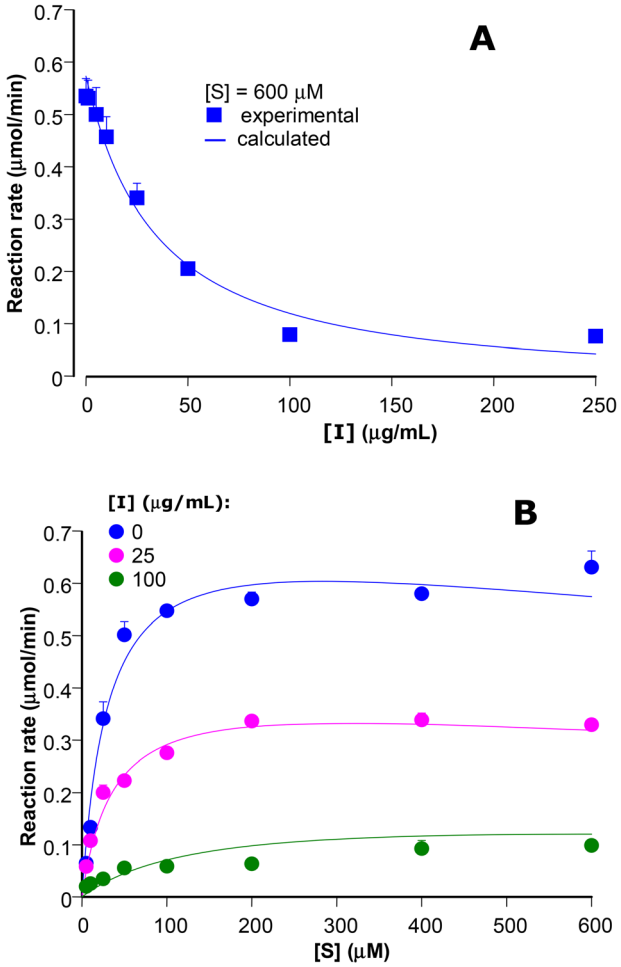

Fig. 5 Reaction rates of the porcine pancreatic lipase obtained by varying simultaneously the concentrations of the *T. indica* seed extract ([I]) and the substrate ([S]; *p*-nitrophenyl-palmitate). (A) Effect concentration dependence; (B) kinect analysis. Each datum point is the mean of four determinations. The lines running through the experimental points were calculated using the optimized parameters obtained by fitting eqn (5) to the experimental data by means of a nonlinear least-squares procedure. The optimized parameters were: K_M, 30.18 ± 2.25 μM; V_{max}, 0.731 ± 0.047 μmol min^{-1}; $\tilde{K}_{i1}$, 22.98 ± 3.42 μg mL^{-1}; K_{i2}, 31.83 ± 3.47 μg mL^{-1}; K_{iS} = 2680.0 ± 1032.3 μM. Goodness of fit indicators were: sum of squared deviations, 0.022; MSC, 3.915; correlation, 0.992.

enzyme was measured as a function of the tamarind extract concentrations. Neither the peel nor the leaf extract inhibited the lipase activity (data not shown). The seed extract, however, was inhibitory. Panel A in Fig. 5 allows the appreciation of the concentration dependence of this inhibition when the substrate (*p*-nitrophenyl-palmitate) concentration was fixed at 600 μM. The IC_{50} value derived from the experimental data by numerical extrapolation was equal to 31.5 μg mL^{-1}.

In order to characterize further the inhibition of lipase by the tamarind seed extract, the activity of the enzyme was measured at various substrate and inhibitor concentrations. The saturation curves in panel B of Fig. 5 were progressively lowered as the seed extract was added in progressively higher concentrations. The possibility of competitive inhibition is disproved because the curves present no tendency to converge at high substrate concentrations. Signs of substrate inhibition at high concentrations are apparent, however, confirming previous reports.[31] Search for the most appropriate kinetic model for describing the data in Fig. 6 arrived at the following equation:

$$v = \frac{V_{max}[S]}{K_M\left(1+\frac{[I]^2}{(\tilde{K}_{i1})^2}\right)+[S]\left(1+\frac{[I]}{(K_{i2})}\right)\left(1+\frac{[S]}{(K_{iS})}\right)}. \quad (6)$$

Besides V_{max} and K_M, whose meanings have already been explained above, K_{iS} is the substrate inhibition constant that was introduced due to the small but significant substrate inhibition. $\tilde{K}_{i1}$ and K_{i2} are the inhibitor constants, and their position means that inhibition is of the mixed type, with the for-

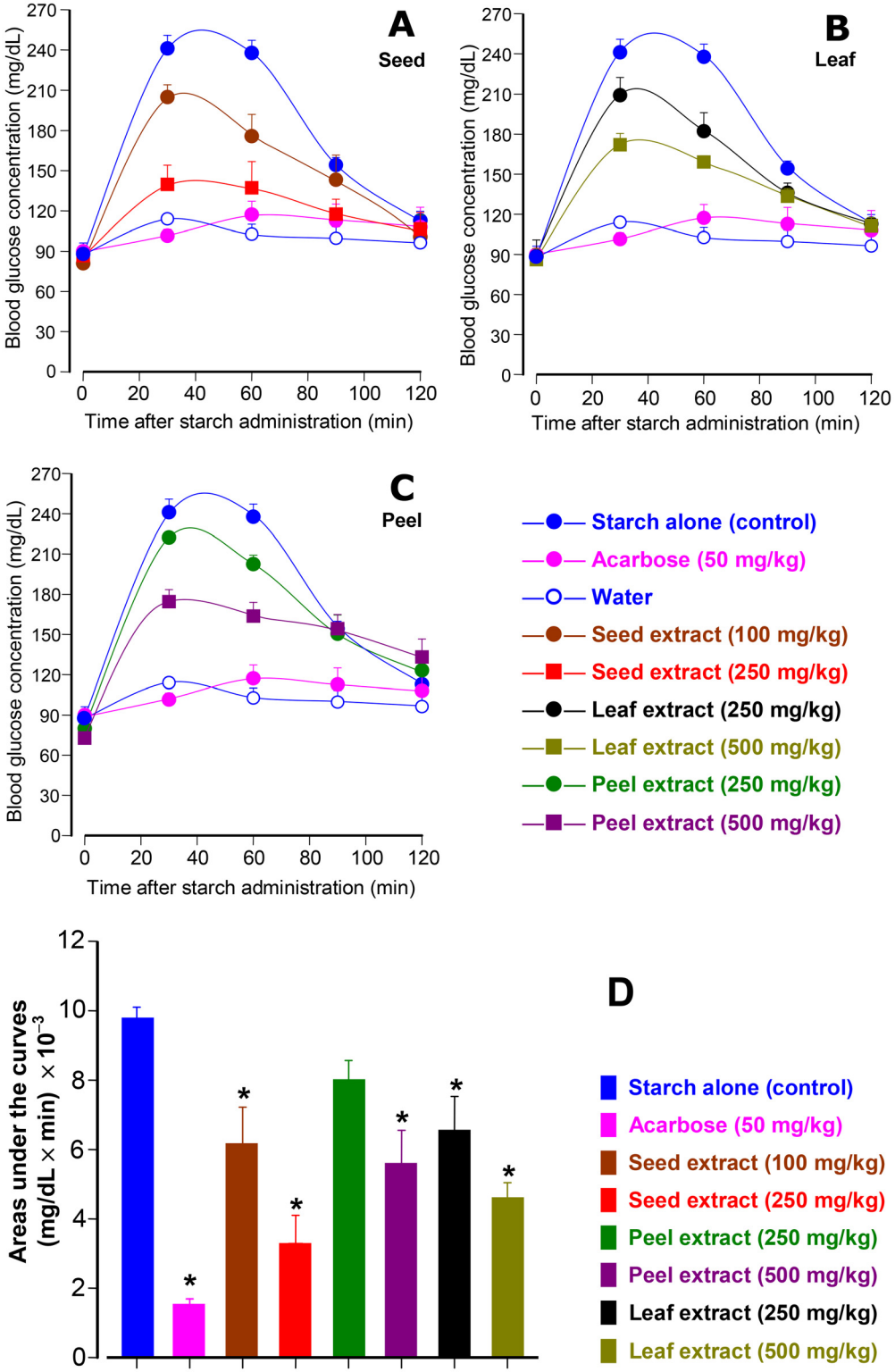

Fig. 6 Effects of extracts prepared from various tamarind parts, seed (A), leaf (B) and peel (C), on blood glucose levels after oral starch administration in mice. The oral administration of commercial starch (1 g per kg body weight) was done immediately after the administration of the extracts or acarbose (reference inhibitor). The doses of each extract are given on the graphs. Plasma glucose was measured as described in the Materials and methods section. Each value represents the mean ± mean standard error of 3–8 mice. (D) shows the areas under the curves obtained for each of the various conditions shown in (A–C), subtracted from the area under the curve obtained after water administration. Asterisks indicate statistical significance relative to the control curve ($p \leq 0.05$).

mation of the EI_2 and ESI complexes. The quadratic term in the denominator denotes parabolic inhibition due to the apparent ability of the free enzyme to accommodate at least two inhibitor molecules at the same time, an ability that is lost when the substrate binds to the enzyme. In the legend of Fig. 5, the values of the optimized kinetic constants are given. The optimized values of $\bar{K}_{i1}$ and K_{i2} are close to the IC_{50} value, but $\bar{K}_{i1} < K_{i2}$, denoting that the EI_2 forms somewhat more readily than the ESI complex, although the difference is not very pronounced. Examination of both panels in Fig. 5, finally, reveals a relatively good agreement between theory and experiment in relation to both *v versus* [I] and *v versus* [S] relationships.

3.4. Summarizing remarks about the kinetic analyses

The kinetic analyses that were done in order to characterize the inhibitions of α-amylase and lipase are useful because they allow the determination of the inhibition constants of each extract. Due to the heterogeneity of the extracts, the determined inhibition constants are certainly complex functions of several individual dissociation constants, but still a measure of the strength of the preparation that was used in terms of its mass. It should be remarked that the heterogeneity of the extract that was used does not invalidate the various equations that were fitted to the data, provided that the proportions between the concentrations of the active compounds are not modified, a condition that holds for extracts with constant composition.[28,31] An advantage of the determination of the kinetic constants, especially the value of the various inhibition constants, is that reliable predictions can be made concerning any combination of substrate and inhibitor concentrations, as illustrated by the demonstration that both the *v versus* [I] and *v versus* [S] relationships can be foreseen with fair confidence. For all extracts, no competitive inhibition was detected, but multiple binding was found for the seed extract components to both α-amylase and lipase. In the case of the α-amylase inhibition by the leaf extract, uncompetitive inhibition was found, a mechanism that represents a relatively rare phenomenon among the inhibitors of this enzyme.

3.5. Effects of the α-amylase inhibitors on the glycemic levels after starch or glucose administration to mice

To evaluate the effectiveness of the tamarind extracts as inhibitors of α-amylase *in vivo*, experiments were performed in which blood glucose levels were quantified at various times after the administration of commercial corn starch. The mean results of these experiments are shown in Fig. 6. The control curve (starch administration alone) showed the usual typical increase in blood glucose levels with maximal values between 30 and 60 minutes after starch administration. All extracts diminished the increases in the glucose levels that followed starch administration. This effect was dose- and extract-dependent, the seed extract being the most effective one. The highest dose of the seed extract (250 mg kg^{-1}) caused an inhibition that was not very far from that one caused by acarbose (50 mg kg^{-1}) – the classical inhibitor of starch absorption. For the other extracts (leaf and peel), even doses as high as 500 mg kg^{-1} produced only partial inhibition. Panel D in Fig. 6 facilitates comparison because the time variable was eliminated. The bars show the areas under the curves, which have been considered an indicator of the starch absorption capacity. The seed extract reduced the area under the curve by 68.6% at the dose of 250 mg kg^{-1}. Numerical interpolation predicts an ID_{50} of 151.4 mg kg^{-1}. At this dose of 250 mg kg^{-1}, the peel extract caused no significant diminution, but the leaf extract was already effective. When the doses were increased to 500 mg kg^{-1}, diminutions of 52.7 and 42.8% were found for the leaf and peel extracts, respectively.

Starch hydrolysis is essential to its digestion, but glucose entry into the systemic circulation also depends on transport systems located in the intestinal cells (enterocytes). In order to investigate the possible action of the extracts on the glucose transporters, a glucose load (1.5 mg kg^{-1}) was administered to mice, and blood glucose levels were quantified along the following time periods. The results are represented in Fig. 7. The doses of the extracts that were given were within the same range as those given for investigating starch absorption. The results reveal no statistically significant compromise of glucose transport across the enterocyte by the extracts even though there seems to be some tendency toward inhibition.

3.6. Effects of the lipase inhibitors on the triglyceride levels after olive oil administration in mice

Considering that the seed extract inhibited the pancreatic lipase *in vitro*, its *in vivo* effectiveness was evaluated through the traditional olive oil tolerance test. In this test, olive oil oral administration is followed by the assay of the excess triglycerides in plasma. Fig. 8A illustrates the time courses of the changes in plasma triglycerides after olive oil (5 mL kg^{-1}) administration under various conditions. The control curve (only olive oil administration) showed a clear rise in the triglyceride levels after olive oil administration, which remained elevated up to 270 minutes following administration. As expected, orlistat administration blocked the rise in plasmatic triglycerides. The extract diminished the rise in triglyceride levels in a concentration-dependent way. Panel B in Fig. 8 allows the comparison of the areas under the triglyceride curves. The diminution of the area, compared to the control, was equal to 54.6% for the 250 mg kg^{-1} dose and 73.9% for the 500 mg kg^{-1} dose. Numerical interpolation predicts a 50% diminution at the dose of 214.9 mg kg^{-1}.

3.7. Summarizing remarks about the effects on starch and triglyceride digestion

Inhibition of starch digestion by the extracts, especially by the seed extracts, is most probably the consequence of the inhibition of pancreatic α-amylase. This conclusion is based on well-established knowledge which states that previous hydrolysis of starch is essential for the absorption process. An inhibition of α-glucosidase is equally possible, but there is evidence that this enzyme is unlikely to be a rate-limiting step for the whole process of starch digestion.[51] Other observations in

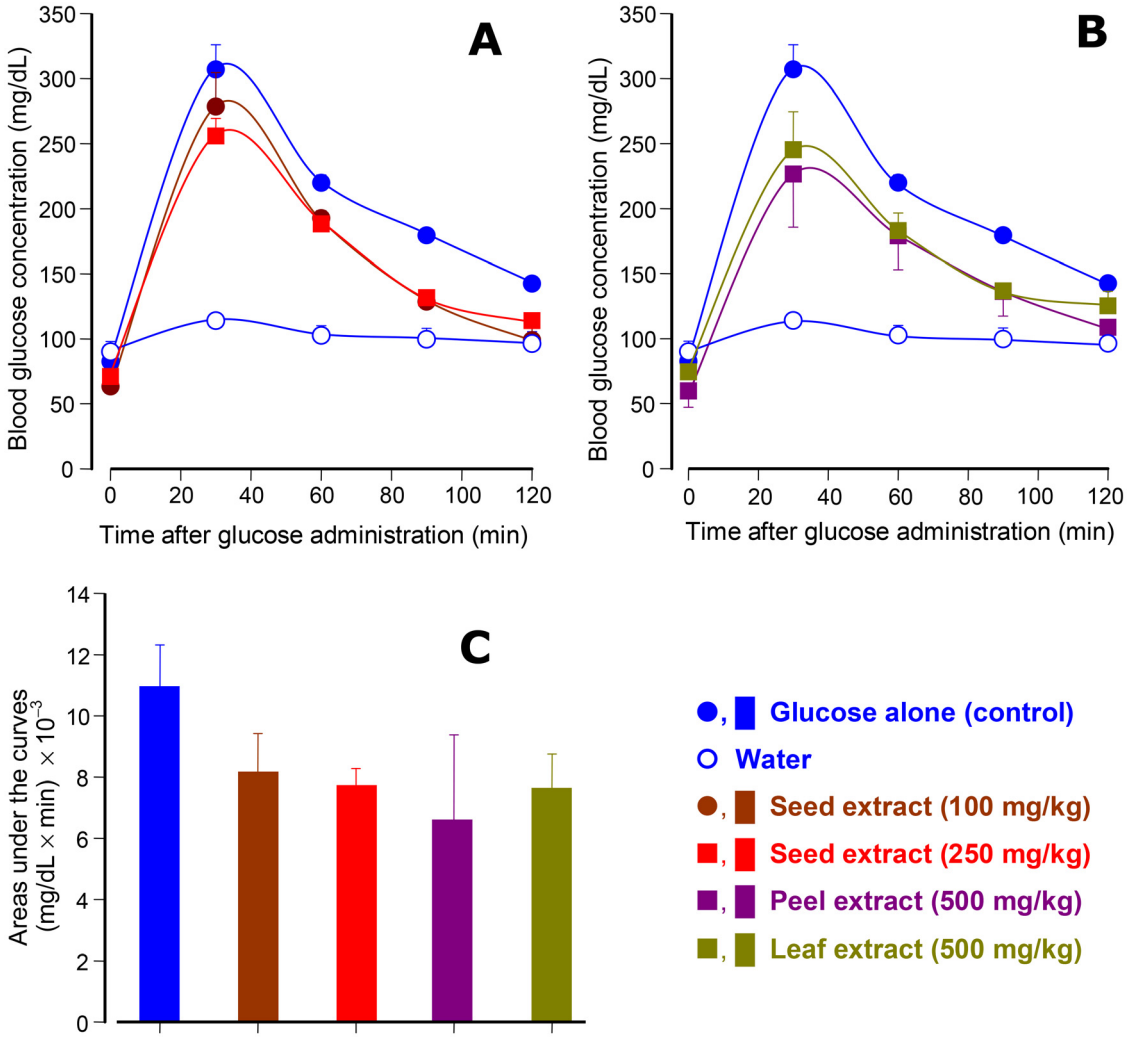

Fig. 7 Effects of extracts prepared from various tamarind parts, seed (A), leaf and peel (B), on blood glucose levels after oral glucose administration in mice. The oral administration of glucose (1.5 g per kg body weight) was done immediately after the administration of the extracts. The doses of each extract are given on the graphs. Plasma glucose was measured as described in the Materials and methods section. Each value represents the mean ± mean standard error of 3 mice. (C) shows the areas under the curves obtained after extract administration shown in (A) and (B), subtracted from the area under the curve obtained after water administration. Asterisks indicate statistical significance relative to the control curve ($p \leq 0.05$).

this study fully corroborate the role of α-amylase inhibition. Firstly, the seed extract was markedly the strongest inhibitor of the enzyme. Consequently, it should also be the strongest inhibitor of starch absorption, a hypothesis that was plainly confirmed. Second, a possible contribution of free glucose absorption[52] was revealed to be improbable or at least very small as no statistically significant modifications of the glucose tolerance curves were found.

Similarly to what was concluded above regarding the inhibition of the pancreatic α-amylase, the inhibition of the pancreatic lipase by the seed extract is the most probable phenomenon behind its action on triglyceride absorption. As mentioned in the Introduction, inhibition of lipase was already reported, for example, by Buchholz and Melzig (2016).[21] The preparation used by these authors, a peel methanolic extract, however, revealed an IC_{50} of 152 μg mL^{-1}, being thus 4.8 times less potent than the seed extract used in the present study (IC_{50} = 31.5 μg mL^{-1}). It is worth recalling that the peel and leaf extracts of the present study did not inhibit pancreatic lipase.

It is equally worth emphasizing that the abilities of the seed extract in diminishing postprandial hyperglycemia and the elevated levels of triglycerides after fat ingestion seem to be quite similar, as revealed by the computed doses for half-maximal effects, namely 151.4 and 214.9 mg kg^{-1}, respectively. A question that can be formulated is one about the doses of the seed extract that are necessary in humans for significant starch and triglyceride absorption inhibition. A 175 mg kg^{-1} dose (midway between the doses for 50% inhibition of starch and triglyceride absorption) for an individual weighing 75 kg would represent a total dose of 13 g. This looks rather excessive unless the extracts were ingested as part of the daily food ingestion. However, the stipulation of 175 mg kg^{-1} was based on the IC_{50} doses measured in mice. For humans, it would

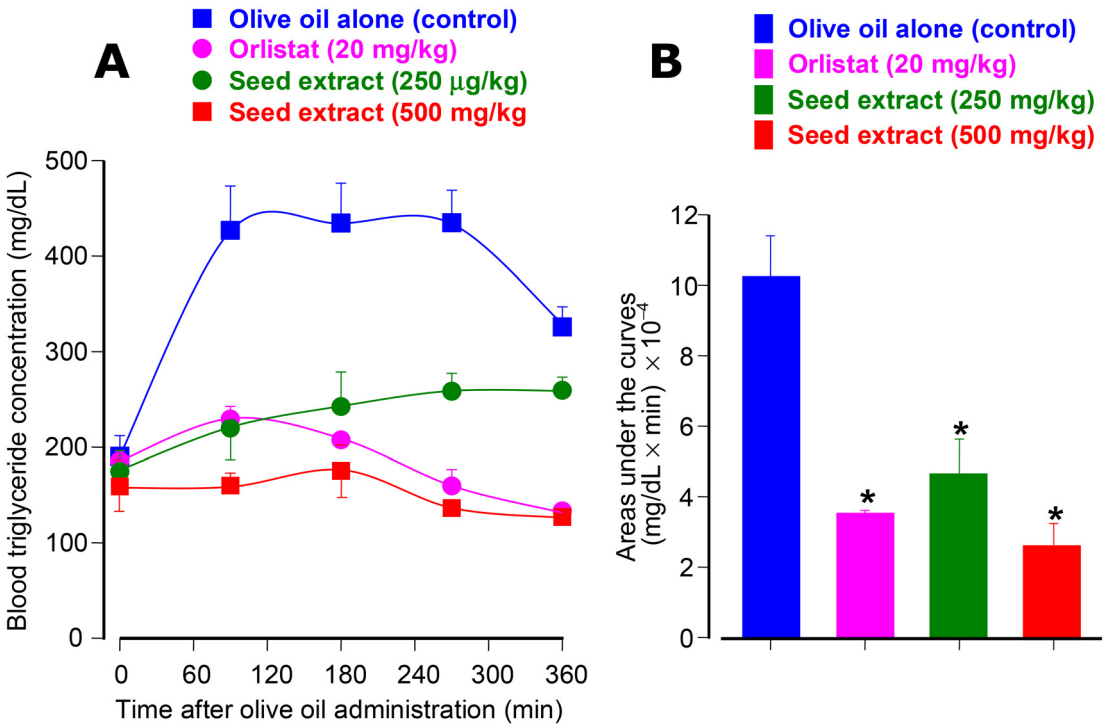

Fig. 8 Effects of tamarind seed extract on blood triglyceride levels after olive oil administration in mice. The oral administration of olive oil (5 mL per kg body weight) was done immediately after the administration of the extracts or orlistat (A). The doses of each extract are given on the graphs. Plasma triglycerides were measured as described in the Materials and methods section. Each value represents the mean ± mean standard error of 3–6 mice. (B) shows the areas under the curves obtained after the various treatments with the tamarind extract shown in (A). Asterisks indicate statistical significance relative to the control curve ($p \leq 0.05$).

perhaps be more appropriate to apply a translation formula.[53] If this is done for the mice at 175 mg kg^{-1} dose, one arrives at a human dose of 14.2 mg kg^{-1}, which represents a total intake of approximately 1 g for an individual weighing 75 kg. This brings a much more favorable perspective, which is indeed worth being investigated in future work.

3.8. Flavonoids, phenolic acids and tannins in the *T. indica* extracts

The various actions of the extracts that were described in the preceding sections are quite frequently attributed to flavonoids, phenolic acids and tannins. For this reason, analytical procedures, long established in our group, were used to separate, identify, and quantify these compounds in the *T. indica* extracts under study. Table 2 presents the contents of the phenolic compounds that were found after redissolving the hydroalcoholic extracts in water. Chromatographic parameters as well as spectral data are also shown. The compounds were identified according to their chromatographic characteristics, ultraviolet light absorption and mass spectra. The table lists forty-three compounds (total phenolics) that can be divided into four groups: phenolic acids, condensed tannins, hydrolysable tannins, and flavonoids. The leaf extract presented the by far highest concentrations of all groups. Half of its phenolics were flavonoids, luteolin-6-*C*-hexoside being the most abundant (37.3% of total flavonoids). The condensed tannins comprised 47.8%, A-type procyanidin pentamer (peak 1), procyanidin trimer (peak 14) and procyanidin tetramer (peak 15) being the most abundant ones. The leaf extract was the only one in which hydrolysable tannins were found, though in small amounts. The seed extract ranked second in terms of the total phenolic compound contents, but this was mainly due to its relatively high content of condensed tannins, which comprised 98.7% of its total phenolics. The main tannins identified in this extract were procyanidin trimer (peaks 3, 4, 6, 8 and 10), procyanidin tetramer (peaks 2, 7, 9, 11, 13, 14, 15 and 16) and B-type (*epi*)afzelech-(*epi*)catechin-(*epi*)catechin (peak 12). The peel extract, finally, had a total phenolic content close to that of the seed extract, but contrary to the latter, it also contained flavonoids (22%) in addition to condensed tannins (76.6%). The most abundant tannins in this extract were procyanidin dimer (peak 9) and procyanidin tetramer (peak 15).

A question that can be formulated is if the flavonoids, phenolic acids and tannins in the extract can be responsible for the inhibitory effects on the α-amylase. It is well established that flavonoids and tannins are inhibitors of both α-amylase and α-glucosidase.[28,51] The three extracts of this study contain such compounds. However, the extract whose content in these substances is the highest, the leaf extract, is much less inhibitory than the seed extract, actually 30 times less potent. Furthermore, the seed extract does not contain flavonoids and its tannin content is very low; according to Table 1, only 1.1%

Table 2 Phenolic profile of the hydroethanolic extracts of tamarind peel, seed, and leaf

Peak	RT (min)	λ_{max} (nm)	$[M-H]^-$ *m/z*	MS^2 (*m/z*)	Tentative identification	Quantification (mg g^{-1})		
						Peel	Seed	Leaf
1	4.18	280	1437	1151 (27), 716 (32), 575 (37), 289 (15), 287 (6)	A-type procyanidin pentamer	nd	nd	3.13 ± 0.03
2	4.27	276	167	123 (100)	Vanillic acid	0.053 ± 0.003	0.114 ± 0.003	nd
3	4.56	278	1153	865 (20), 577 (27), 575 (16), 561 (7), 289 (100)	Procyanidin tretramer	0.336 ± 0.004	0.165 ± 0.004	nd
4	4.75	284	865	451 (44), 425 (59), 407 (97), 289 (65)	B-type procyanidin trimer	0.86 ± 0.05	0.8 ± 0.01	nd
5	4.94	281	865	451 (44), 425 (59), 407 (97), 289 (65)	Procyanidin trimer	0.251 ± 0.004	0.676 ± 0.005	nd
6	5.14	320	353	191 (82), 179 (32), 173 (71), 135 (100)	3-*O*-Caffeoylquinic acid	0.088 ± 0.001	0.074 ± 0.001	0.1241 ± 0.0001
7	5.46	282	865	451 (44), 425 (59), 407 (97), 289 (65)	Procyanidin trimer	0.471 ± 0.004	1.35 ± 0.01	nd
8	5.51	280	1435	1151 (100), 717 (92), 575 (47), 289 (25), 287 (10)	A-type procyanidin pentamer	nd	nd	0.716 ± 0.005
9	5.62	280	577	451 (38), 425 (67), 407 (100), 289 (76), 287 (20)	Procyanidin dimer	1.01 ± 0.04	0.27 ± 0.01	nd
10	6.46	283	865	451 (44), 425 (59), 407 (97), 289 (65)	Procyanidin trimer	nd	nd	0.393 ± 0.005
11	6.72	322	353	191 (100), 179 (24), 173 (37)	5-*O*-Caffeoylquinic acid	nd	nd	0.928 ± 0.001
12	6.88	289	289	245 (100)	(+)-Catechin	0.607 ± 0.003	nd	nd
13	7.05	280	865	451 (44), 425 (59), 407 (97), 289 (65)	Procyanidin trimer	0.76 ± 0.01	1.53 ± 0.05	nd
14	7.39	281	865	451 (44), 425 (59), 407 (97), 289 (65)	Procyanidin trimer	0.269 ± 0.002	nd	2.38 ± 0.02
15	8.03	280	1153	865 (20), 577 (27), 575 (16), 561 (7), 289 (100)	Procyanidin tetramer	1.73 ± 0.04	1.49 ± 0.03	2.7 ± 0.1
16	8.49	280	865	451 (44), 425 (59), 407 (97), 289 (65)	Procyanidin trimer	0.31 ± 0.01	0.85 ± 0.05	nd
17	9.11	280	1153	865 (20), 577 (27), 575 (16), 561 (7), 289 (100)	Procyanidin tetramer	0.179 ± 0.001	0.94 ± 0.02	1.2 ± 0.04
18	9.56	280	849	577 (51), 559 (48), 289 (100), 287 (19)	B-type (*epi*)afzelech-(*epi*)catechin-(*epi*)catechin	0.203 ± 0.003	0.9 ± 0.03	nd
19	9.67	338	593	473 (100), 383 (15), 353 (31)	Apigenin-6-*C*-glucose–8-*C*-glucose	nd	nd	1.35 ± 0.02
20	9.85	280	289	245 (100)	(−)-Epicatechin	nd	nd	2.648 ± 0.04
21	10.21	280	1151	1009 (100), 863 (89), 575 (36), 289 (18)	A-type procyanidin tetramer	0.185 ± 0.004	0.604 ± 0.001	nd
22	10.39	278	1153	865 (20), 577 (27), 575 (16), 561 (7), 289 (100)	Procyanidin tetramer	nd	0.797 ± 0.002	nd
23	11.13	278	1153	865 (20), 577 (27), 575 (16), 561 (7), 289 (100)	Procyanidin tetramer	nd	0.293 ± 0.001	1.55 ± 0.03
24	11.23	281	865	451 (44), 425 (59), 407 (97), 289 (65)	Procyanidin trimer	nd	nd	2.5 ± 0.1
25	12.42	280	1153	865 (20), 577 (27), 575 (16), 561 (7), 289 (100)	Procyanidin tetramer	0.33 ± 0.01	0.599 ± 0.004	nd
26	12.73	339	1235	1083 (100), 781 (62), 601 (12)	Galloyl-punicalagin	nd	nd	0.189 ± 0.002
27	13.05	355	609	301 (100)	Quercetin-3-*O*-rutinoside	0.367 ± 0.003	nd	nd
28	13.22	281	865	451 (44), 425 (59), 407 (97), 289 (65)	Procyanidin trimer	nd	nd	nd
29	13.42	281	577	451 (38), 425 (67), 407 (100), 289 (76), 287 (20)	Procyanidin dimer	0.324 ± 0.003	nd	0.86 ± 0.05
30	13.78	280	577	451 (38), 425 (67), 407 (100), 289 (76), 287 (20)	Procyanidin dimer	0.48 ± 0.003	nd	nd
31	13.84	339	563	545 (45), 473 (100), 443 (11), 425 (67), 413 (18), 383 (21), 353 (12)	Apigenin-6-*C*-pentoside–8-*C*-hexoside	nd	nd	0.315 ± 0.003
32	14.30	328	463	301 (100)	Quercetin-3-*O*-glucoside	0.175 ± 0.001	nd	nd
33	14.49	330	575	531 (33), 429 (38), 411 (100), 367 (65), 357 (15), 337 (20), 309 (10)	Luteolin-*O*-deoxyosyl-6-*C*-(6-deoxy-pento-hexos-ulosyl)	0.49 ± 0.03	nd	nd
34	14.91	332	447	285 (100)	Luteolin-6-*C*-glucoside	0.13 ± 0.003	nd	7.8 ± 0.3
35	15.34	346	1441	1153 (27), 865 (92), 577 (47), 289 (25), 287 (10)	B-type procyanidin pentamer	nd	nd	0.63 ± 0.01
36	16.09	280	1153	865 (20), 577 (27), 575 (16), 561 (7), 289 (100)	Procyanidin tetramer	nd	nd	4 ± 0.1
37	16.54	342	461	299 (100)	Chrysoeriol-7-*O*-hexoside	0.06 ± 0.002	nd	nd
38	16.84	338	431	311 (15), 283 (100)	Hydroxydaidzein-8-*C*-glucoside isomer I	nd	nd	3 ± 0.2
39	17.15	281	863	863 (100), 711 (26), 573 (16), 451 (18), 411 (30), 289 (16), 285 (12)	A-type procyanidin trimer	0.411 ± 0.003	nd	nd
40	18.26	339	431	311 (23), 283 (100)	Hydroxydaidzein-8-*C*-glucoside isomer II	nd	nd	5.8 ± 0.2
41	18.42	330	431	269 (100)	Apigenin-7-*O*-glucoside	0.204 ± 0.003	nd	nd
42	19.26	345	449	287 (100)	Eriodictyol-hexoside	0.136 ± 0.002	nd	nd
43	19.61	330	461	446 (35), 341 (5), 299 (88), 283 (100)	5,5′-Dihydroxy-3′-methoxy-isoflavone-7-*O*-β-glucoside	0.16 ± 0.001	nd	nd

Table 2 *(Contd.)*

Peak	RT (min)	λ_{max} (nm)	$[M-H]^-$ *m/z*	MS^2 (*m/z*)	Tentative identification	Quantification (mg g^{-1})		
						Peel	Seed	Leaf
					Total phenolic acid	0.141 ± 0.003	0.188 ± 0.003	1.052 ± 0.002
					Total flavonoids	2.33 ± 0.05	nd	21 ± 1
					Total condensed tannins	8.1 ± 0.2	11.3 ± 0.2	20.1 ± 0.4
					Total hydrolisable tannins	nd	nd	0.189 ± 0.002
					Total phenolic compounds	10.6 ± 0.2	11.45 ± 0.22	42 ± 1

RT: retention time; nd: not detected. Calibration curve used: catechin ($y = 84950x - 23\,200$, $R^2 = 0.9999$; LOD 0.17 μg mL^{-1}; LOQ 0.68 μg mL^{-1}); chlorogenic acid ($y = 168823x - 161\,172$; $R^2 = 0.9999$; LOD = 0.20 μg mL^{-1}; LOQ = 0.68 μg mL^{-1}); quercetin 3-*O*-glucoside ($y = 34843x - 160\,173$; $R^2 = 0.9998$; LOD = 0.21 μg mL^{-1}; LOQ = 0.71 μg mL^{-1}); apigenin 6-*C*-glucoside ($y = 107025x - 61\,531$; $R^2 = 0.9989$; LOD = 0.19 μg mL^{-1}; LOQ = 0.63 μg mL^{-1}); apigenin 6-*C*-glucoside ($y = 107025x - 61\,531$; $R^2 = 0.9989$; LOD = 0.19 μg mL^{-1}; LOQ = 0.63 μg mL^{-1}); daidzin ($y = 27\,652x + 29\,187$, $R^2 = 0.9996$, LOD = 2.05 μg mL^{-1}; LOQ = 6.23 μg mL^{-1}); gallic acid ($y = 131538x + 292\,163$, $R^2 = 0.9969$, LOD = 8.05 μg mL^{-1} and LOQ = 24.41 μg mL^{-1}); 4-hydroxybenzoic acid ($y = 208604x + 173\,056$, $R^2 = 0.9988$, LOD = 0.29 μg mL^{-1}; LOQ = 0.83 μg mL^{-1}).

of the extract corresponds to tannins. This means that the extract concentration that caused 50% inhibition of the α-amylase, 13.3 μg mL^{-1}, contained not more than 0.15 μg tannins per mL. This is really a very low tannin concentration, whose contribution to the α-amylase inhibition was most likely small. A similar reasoning applies to the doses that were given to the mice and that inhibited starch absorption. The 250 mg kg^{-1} dose of the seed extract inhibited starch absorption by 68.6%. The corresponding dose of tannins that was given to these animals in these experiments was equal to 2.82 mg kg^{-1} if one takes into account the contents in Table 2. In all studies published up to now, much higher concentrations and doses of tannins are required for significant inhibition of α-amylase activity and starch absorption. For example, 50% inhibition of the α-amylase by a condensed tannin was reported to occur at concentrations around 200 μg mL^{-1}, and the corresponding effect on starch absorption required doses of 100 mg kg^{-1}.[28] If the same calculations are applied to the leaf extract, the results are more favorable to the participation of flavonoids and tannins as inhibitors of the α-amylase. Inhibition of this enzyme by the leaf extract revealed an IC_{50} value around 500 μg mL^{-1}. This leaf extract concentration corresponds to 1.76 μg mL^{-1} flavonoids + tannins, *i.e.*, an 11.7 times higher concentration than the one in the seed extract that produced 50% inhibition of the α-amylase. Similarly, a leaf extract dose of 500 mg kg^{-1}, which reduced starch digestion in mice by approximately 50% (see Fig. 6), corresponds to a flavonoids + tannins dose of 21 mg kg^{-1}. This is a dose that can be expected to contribute significantly to starch digestion inhibition if one takes into account the literature reports.[51,54] In the case of the leaf extract, thus, the contribution of the compounds listed in Table 2 for the α-amylase inhibition was considerably more important than that for the seed extract.

Similar to what was discussed concerning the effects on starch absorption, tannins are the most likely candidates for inhibiting pancreatic lipase if one looks at the data in the literature.[32] However, the absence of effects on pancreatic lipase by the leaf extract, which contains more tannins than the seed extract, does not favor this hypothesis. Furthermore, literature reports indicate that the concentrations and doses of tannins that are required are not compatible with the low contents in these compounds of the extracts used in the present study. For example, if the seed extract dose that produces 50% inhibition of triglyceride absorption was given to mice, namely 214.9 mg kg^{-1}, the administered dose of tannins would be equal to 2.43 mg kg^{-1}. This is a low dose, and it would require a very high inhibitory power, which has not yet been reported for tannins.[32] Clearly, also in this case, although the compounds listed in Table 2 certainly contribute to some extent to the inhibition of fat absorption seen in the present work, they are unlikely to be the sole responsible agents.

3.9. Further chemical analyses of the *T. indica* extracts

The indication that other compounds in addition to flavonoids, phenolic acids and tannins are likely to be involved in the inhibitory effects of the various extracts on the activities of

α-amylase and pancreatic lipase prompted us to search for the presence of additional compounds. Considering that the seed extract was the by far most potent inhibitor of the α-amylase and pancreatic lipase, our interest was centered on finding compounds that are unique for this extract. The results of the qualitative UHPLC-ESI(−/+)-MS/MS analysis, which are shown in Table 3, revealed a total of 68 different compounds. The tentative identification was based on comparisons of the MS and MS/MS spectra with those available in public databases such as GNPS, Mass Bank, and HMDB, along with the literature data.[55–57]

Although quantification was not possible, a comparison of the compounds found in the various extracts reveals some useful characteristics that may help in discerning potential molecular entities that could be involved in the superior inhibitory effects of the seed extract on α-amylase and lipase. A total of 19, 34, and 48 compounds were detected in the seed, peel, and leaf extracts, respectively. Similar entities include amino acids, sugars, alcohols and polyols, carbohydrates, flavonoids, organic acids, alkaloids, hydroxycinnamic and linoleic acids, fatty acids, steroids and steroid derivatives, amines, and vitamins. When comparing the extracts, the leaf extract contained a higher diversity of amino acids than the other extracts. The peel extract revealed the lowest diversity of flavonoids. The 19 chemical entities of the seed extract were almost equally distributed over the various categories. However, some compounds were unique to the seed extract, including lenticin, masoprocol, chenodeoxycholic acid, ursodiol and 13-keto-9*Z*,11*E*-octa-decadienoic acid (KOC).

One of the questions that was formulated above was the apparent discrepancy between the total phenolic contents determined by means of the Folin–Ciocalteu method shown in Table 1 and the phenolic compounds that were quantified chromatographically and displayed in Table 2. The former method revealed the highest content in phenolic groups for the seed extract when compared to the other extracts, whereas the chromatographic quantification favoured in this respect the leaf extract. It is well known that the Folin–Ciocalteu method for phenolic group determination is subject to many interferences as its application usually results in higher phenolic contents than those quantified when individual separations of flavonoids, phenolic acids and tannins are performed.[49,50] The list of interfering compounds is very long and it includes amino acids and carboxylic acids, for example.[50] The presence of several compounds, including amino acids and carboxylic acids in the extracts, was indeed corroborated by the qualitative UHPLC-ESI-MS/MS analysis (Table 3) in the same lyophilized extracts. On the other hand, the way by which the extracts were resolubilized may have influenced the compounds that were available for actual detection. In fact, water was used to solubilize the extracts before the HPLC-DAD-ESI/MSn analysis (Table 2), whereas a 1 : 1 mixture of water and acetonitrile was the solvent used in the qualitative UHPLC-ESI(−/+)-MS/MS analysis (Table 3). Since the samples were filtered before the analyses, differences in solubility may have generated samples with different compositions. Consequently, although the chromatographic quantification shown in Table 2 reveals several of the flavonoids, phenolic acids and tannins also found in the qualitative UHPLC-ESI(−/+)-MS/MS analysis, such as procyanidins, epicatechin and others, the latter technique was notable in that it revealed the presence of several potential antioxidant molecules in the seed extract that display phenolic groups and that are absent in other extracts. One such compound is lenticin, also known as hypaphorine, a L-tryptophan-derived alkaloid that exhibits antioxidant properties in various cellular models. Its antioxidant activity results from its ability to effectively scavenge DPPH radicals.[58] Another compound, masoprocol, also known as nordihydroguaiaretic acid, also exhibits notable antioxidant properties even at low concentrations.[59] These specific compounds present in the seed extract could be responsible not only for the antioxidant activity but also for the inhibitory effect on the α-amylase and lipase, as will be discussed below.

3.10. *In silico* studies

As discussed above, the chemical composition of the tamarind seed extract is quite complex (Tables 2 and 3). Testing of isolated molecules from the extract for their effects on the α-amylase and lipase activities is quite challenging because it requires the substances in pure form. Actually, several flavonoids, phenolics and tannins have already been tested.[28,54,60,61] However, as argued above, it seems unlikely that they are the main α-amylase and lipase inhibitors of the seed extract due to their limited presence. Given this, it seems more reasonable to direct efforts on the unique components that were identified in the qualitative UHPLC-ESI(−/+)-MS/MS analysis. These substances are not available in pure form, so the experiments cannot be done. Then, the most convenient approach would be to infer initially from computer simulations their potential as inhibitors of α-amylase and lipase, as it was already done for several flavonoids, phenolics and tannins.[29,48,54,60]

Re-docking simulations were employed as an initial strategy to evaluate the performance of docking programs and protocols. This method involves the docking of a ligand already present in a crystallographic or modeled structure four times per program. In this sense, acarbose and MUP were re-docked to α-amylase and lipase, respectively, and the results are summarized in Table S1 and Fig. S3†, which reproduced in the best pose that matches the modelled/crystallographic one in all repetitions. The Root Mean Square Deviation (RMSD) values, which measure the stability and accuracy of the docking poses, were maintained below 2 Å. This threshold indicates high confidence in the precision of the docking results.[46,47] To make the selection criterion even more stringent, the reference molecule should exhibit the same pose on protein binding in all replicates by all programs. Successful re-docking simulations indicate that the docking protocol can be used to assess unknown ligands from a virtual library. Thus, the docking protocols were applied to evaluate the effects of specific molecules present in the tamarind seed extract according to the virtual library composed of 19 molecules identified by UPLC-MS. To

Table 3 Qualitative chemical analysis of the hydroethanolic extracts of tamarind peel, seed, and leaf

Metabolite	Retention time	Formula	Mono mass	[M + H] theoretical	[M + H] experimental	Δ ppm	Adduct	Leaf	Peel	Seed
Amino acids										
Arginine	0.87	$C_6H_{14}N_4O_2$	174.1116	173.1033	173.1041	4.621518	$[M-H]$	x	x	
L-Histidine	0.93	$C_6H_9N_3O_2$	155.0694	154.0611	154.0617	3.894559	$[M-H]$	x		
Pyroglutamic acid	1.15	$C_5H_7NO_3$	129.0425	130.0498	130.0489	−6.92043	$[M+H]$	x	x	x
Glutamine	1.17	$C_5H_{10}N_2O_3$	146.0691	147.0764	147.0754	−6.92837	$[M+H]^+$	x	x	
Asparagine	1.17	$C_4H_8N_2O_3$	132.0534	131.0451	131.046	6.867865	$[M-H]$	x		
D-(−)-Glutamic acid	1.21	$C_5H_9NO_4$	147.0531	146.0447	146.0455	5.477775	$[M-H]$	x		
Phenylalanine	4.57	$C_9H_{11}NO_2$	165.0789	166.0862	166.0853	−5.41887	$[M+H]$	x		
Betaine	6.77	$C_5H_{11}NO_2$	117.0789	118.0862	118.0854	−6.77471	$[M+H]^+$	x		
L-Tryptophan	7.13	$C_{11}H_{12}N_2O_2$	204.0898	203.0815	203.0819	1.969653	$[M-H]$	x		
Lenticin	8.47	$C_{14}H_{18}N_2O_2$	246.1368	247.1441	247.1425	−6.47396	$[M+H]^+$			x
Phenylacetylaspartic acid	11.64	$C_{12}H_{13}NO_5$	251.0793	250.0709	250.0715	2.39932	$[M-H]$	x		
Tryptophan	12.38	$C_{11}H_{12}N_2O_2$	204.0898	205.0976	205.0958	−8.77631	$[M+H]^+$	x		
Vitamins										
Pyridoxine	1.16	$C_8H_{11}NO_3$	169.0738	170.0811	170.0798	−7.64341	$[M+H]$	x		
Sugars and carbohydrates										
Trehalose	1.17	$C_{12}H_{22}O_{11}$	342.1162	341.1078	341.1082	1.17265	$[M-H]$	x	x	x
Sucrose	1.27	$C_{12}H_{22}O_{11}$	342.1162	325.1128	325.1111	−5.33661	$[M+H-H_2O]$	x	x	x
Gluconic acid	1.31	$C_6H_{12}O_7$	196.0583	195.0499	195.0508	4.614204	$[M-H]$	x	x	x
Organic and carboxylic acids										
Malate	2.05	$C_4H_4O_5^{-2}$	132.0058	133.0131	133.0137	4.510834	$[M+H]$	x	x	
(*S*,*S*)-Tartaric acid	2.24	$C_4H_6O_6$	150.0164	149.008	149.0087	4.697734	$[M-H]$	x	x	
Citric acid	3.4	$C_6H_8O_7$	192.027	191.0186	191.0192	3.141055	$[M-H]$	x		x
Alcohols and polyols										
D-(−)-Quinic acid	1.7	$C_7H_{12}O_6$	192.0633	191.055	191.0557	3.663866	$[M-H]^-$	x	x	
Chlorogenic acid	10.64	$C_{16}H_{18}O_9$	354.095	355.1023	355.1004	−5.35057	$[M+H]$	x		
Phenols and related compounds										
Pyrogallol	1.28	$C_6H_6O_3$	126.0316	127.0389	127.038	−7.08444	$[M+H]$	x	x	
Benzoic acid	9.57	$C_{13}H_{16}O_9$	316.0794	315.071	315.071	0	$[M-H]$	x		
6,7-Dihydroxycoumarin	13.6	$C_9H_6O_4$	178.1488	177.0182	177.0182	0	$[M-H]$		x	
Flavonoids and derivatives										
Procyanidin B2	9.77	$C_{30}H_{26}O_{12}$	578.1424	577.134	577.1343	0.51981	$[M-H]$	x	x	x
(−)-Epicatechin	10.53	$C_{15}H_{14}O_6$	290.079	289.0706	289.0704	−0.69187	$[M-H]$	x	x	
Apigenin	10.53	$C_{15}H_{10}O_5$	290.079	289.0706	289.0704	−0.69187	$[M-H]$	x	x	
Epicatechin	10.57	$C_{15}H_{14}O_6$	290.079	291.0863	291.085	−4.46603	$[M+H]$	x	x	
Isoorientin	12.36	$C_{21}H_{20}O_{11}$	448.1005	447.0921	447.0908	−2.90768	$[M-H]$	x		
Orientin	12.38	$C_{21}H_{20}O_{11}$	448.1005	449.1078	449.105	−6.23458	$[M+H]$	x		
Taxifolin	12.76	$C_{15}H_{12}O_7$	304.0583	303.0499	303.0504	1.649893	$[M-H]$		x	
Dihydrokaempferol	14.33	$C_{15}H_{12}O_6$	288.0633	287.055	287.0549	−0.34837	$[M-H]$		x	
Vitexin	14.82	$C_{21}H_{20}O_{10}$	432.1056	431.0972	431.0966	−1.3918	$[M-H]$	x		
Tectoridin	14.87	$C_{22}H_{22}O_{11}$	462.1162	461.1078	461.1071	−1.51808	$[M-H]^-$		x	
Aromadendrin	15.61	$C_{15}H_{12}O_6$	288.0633	289.0706	289.0695	−3.8053	$[M+H]$		x	
Genistein	15.69	$C_{15}H_{10}O_5$	270.0528	271.0601	271.0586	−5.53383	$[M+H]^+$	x	x	
7,4′-Dihydroxyflavone	17	$C_{15}H_{10}O_4$	254.0579	253.0495	253.0497	0.790359	$[M-H]^-$	x	x	
Kaempferol	17.34	$C_{15}H_{10}O_6$	286.0473	287.0551	287.0533	−6.27057	$[M+H]^+$	x	x	
Eriodictyol	15.53	$C_{15}H_{12}O_6$	288.0633	287.055	287.0548	−0.69673	$[M-H]$		x	
Luteolin	17.4	$C_{15}H_{10}O_6$	286.0477	285.0393	285.0393	0	$[M-H]^-$	x	x	
Naringenin	17.06	$C_{15}H_{12}O_5$	272.0684	271.0601	271.0603	0.737844	$[M-H]^-$		x	
Kaempferide	18.56	$C_{16}H_{12}O_6$	300.0633	299.055	299.0548	−0.66877	$[M-H]$		x	
Flavonoid glycosides										
Saponarin	11.17	$C_{27}H_{30}O_{15}$	594.1584	593.15	593.1505	0.842957	$[M-H]$	x		
Isoorientin	12.38	$C_{21}H_{20}O_{11}$	448.1005	449.1078	449.1056	−4.8986	$[M+H]$	x		
Alkaloids and derivatives										
Trigonelline	1.27	$C_7H_7NO_2$	137.0476	138.0549	138.0539	−7.2435	$[M+H]^+$	x		x
Cyclohexane compounds and derivatives										
Myo-inositol	1.12	$C_6H_{12}O_6$	180.0633	179.055	179.0552	1.116975	$[M-H]$	x	x	x
Chlorogenic acid	10.66	$C_{16}H_{18}O_9$	354.095	353.0867	353.0863	−1.13287	$[M-H]^-$	x		
Nitrogenous compounds										
Phosphocholine	1.24	$C_5H_{15}NO_4P^+$	184.0738	184.0738	184.0722	−8.69217	$[M]^+$	x	x	
N-Methylisoleucine	1.33	$C_7H_{15}NO_2$	145.1102	144.1019	144.1008	−7.63349	$[M-H]^-$	x	x	x
Phytosphingosine	20	$C_{18}H_{39}NO_3$	317.2929	318.3002	318.299	−3.77003	$[M+H]$	x	x	
Benzene derivative										
Masoprocol	15.6	$C_{18}H_{22}O_4$	302.1518	301.1434	301.1451	5.645151	$[M-H]^-$			x
Fatty acids and derivatives										
2-Isopropylmalic acid	10.45	$C_7H_{12}O_5$	176.0684	175.0601	175.0606	2.856162	$[M-H]$	x		
Lauryldiethanolamine	13.13	$C_{16}H_{35}NO_2$	273.2667	274.274	274.2714	−9.47957	$[M+H]$	x	x	x
Hydron; nonanedioate	15.34	$C_9H_{16}O_4$	188.1048	187.0964	187.0971	3.741387	$[M-H]^-$	x		
Octadecanoic acid	17.35	$C_{18}H_{36}O_2$	284.2715	283.2631	283.2619	−4.23634	$[M-H]$		x	

Table 3 *(Contd.)*

Metabolite	Retention time	Formula	Mono mass	[M + H] theoretical	[M + H] experimental	Δ ppm	Adduct	Leaf	Peel	Seed
Ceratodictyol	18.27	$C_{19}H_{38}O_4$	330.277	331.2842	331.281	−9.65938	[M + H]	x	x	x
9(10)-Epome	20.27	$C_{18}H_{32}O_3$	296.2351	279.2319	279.23	−6.80438	[M + H − H_2O]	x	x	x
Steroids and derivatives										
Chenodeoxycholic acid	20.66	$C_{24}H_{40}O_4$	392.2926	375.2894	375.2875	−5.06276	[M + H − H_2O]			x
Ursodiol	20.66	$C_{24}H_{40}O_4$	392.2926	391.2842	391.2841	−0.25557	$[M - H]^-$			x
Benzofurans										
Loliolide	12.86	$C_{11}H_{16}O_3$	196.1099	197.1172	197.1163	−4.56581	[M + H]	x		
Linolic acids										
9-OxoOTrE	15.98	$C_{18}H_{28}O_3$	292.2038	293.2111	293.2085	−8.86733	[M + H]	x		
13*S*-HOT	18.87	$C_{18}H_{30}O_3$	294.2194	277.2162	277.2158	−1.44292	[M + H − H_2O]	x		x
9(*S*)-HODE	20.17	$C_{18}H_{32}O_3$	296.2351	295.2267	295.2268	0.338723	$[M - H]^-$	x		x
13-Keto-9*Z*,11*E*-octadecadienoic acid	20.25	$C_{18}H_{30}O_3$	294.2194	295.2267	295.2245	−7.4519	[M + H]			x
Hydroxycinnamic acids										
Coumaroyl hexoside	9.99	$C_{15}H_{18}O_8$	326.1001	325.0917	325.0915	−0.61521	[M − H]	x		
Caffeicacid	10.67	$C_9H_8O_4$	180.0422	163.0386	163.038	−3.68011	[M + H − H_2O]	x		
9-HOTrE	21.23	$C_{18}H_{30}O_3$	294.2194	293.2111	293.2108	−1.02315	[M − H]	x		

select the most promising ligands, we considered not only score values of anchoring (MRS), but also the reproducibility in all repetitions using the described programs. Since each one uses a distinct set of algorithms to predict binding poses and scores, when different programs can reproduce a similar result repeatedly it is more likely that they are true positives. Molecular docking accurately predicts ligand–protein binding and estimates binding strength from docking scores.[46,47] The best the virtual screening results are displayed in Table 4, while the structures of the compounds and reference molecules are presented in Fig. S4 and Fig. S5 respectively.†

According to Table 4, among the nineteen compounds identified in the tamarind seeds, six showed a MRS close to the reference inhibitor acarbose, suggesting a potential interaction of these compounds with the catalytic site of the pancreatic α-amylase. Four of them are unique to the seed extract according to Table 3, namely masoprocol, chenodeoxycholic acid, ursodiol and lenticin. 13(*S*)HOT was also found in the leaf extract and procyanidin B2 in all extracts analyzed. The latter belongs to the group of procyanidins for which several structures have been quantified according to the data in Table 2. It must be remarked that the MRS of procyanidin B2 was very close to that of acarbose and previous publications have indeed reported strong inhibition of α-amylase by this compound with an IC_{50} value of 3.8 μg mL^{-1} and AutoDock Vina scores close to those obtained in the current study.[62]

Table 4 Mean relative docking scores of six molecules selected from virtual screening of the *Tamarindus indica* seed extract. The reference crystallographic ligand acarbose (1XD0) and methoxyundecylphosphinic acid (MUP, 1LPB) were used as references for α-amylase and lipase (*Homo sapiens*), respectively

Pancreatic α-amylase			
Ligand	AutoDock Vina score (kcal mol^{-1})	Gold score (kcal mol^{-1})	MRS
Acarbose	−8.7 ± 0.075[a]	73.95 ± 1.648[a]	0.991 ± 0.02[a]
Procyanidin B2	−8.5 ± 0.000[b]	71.13 ± 0.442[b]	0.960 ± 0.01[b]
Masoprocol	−7.6 ± 0.000[c]	62.19 ± 0.586[c]	0.849 ± 0.01[c]
Chenodeoxycholic acid	−8.4 ± 0.000[d]	52.36 ± 0.138[d]	0.829 ± 0.00[d]
Ursodiol	−8.0 ± 0.023[e]	53.74 ± 2.049[d]	0.817 ± 0.02[e]
Lenticin	−6.2 ± 0.000[f]	62.75 ± 0.208[c]	0.772 ± 0.02[f]
13(*S*)-HOT	−5.7 ± 0.131[g]	62.75 ± 0.195[c]	0.745 ± 0.01[g]
Pancreatic lipase	**AutoDock 4.2.3 score (kcal mol^{-1})**	**Gold score (kcal mol^{-1})**	**MRS**
Ursodiol	−8.47 ± 0.067[a]	46.94 ± 0.360[a]	0.824 ± 0.00[a]
Masoprocol	−5.85 ± 0.166[b]	65.92 ± 0.499[b]	0.801 ± 0.01[b]
Chenodeoxycholic acid	−8.13 ± 0.218[c]	45.95 ± 0.102[b]	0.797 ± 0.01[b]
Procyanidin B2	−6.33 ± 0.078[b]	59.82 ± 1.718[c]	0.787 ± 0.00[c]
13-Keto-9*Z*,11*E*-octadecadienoic acid	−4.18 ± 0.257[d]	66.30 ± 0.948[b]	0.685 ± 0.02[d]
Ceratodictyol	−3.12 ± 0.077[e]	72.26 ± 1.099[d]	0.684 ± 0.01[d]
Orlistat	−2.65 ± 0.081[e]	70.12 ± 0.062[d]	0.641 ± 0.00[e]
MUP	−3.81 ± 0.135[f]	53.30 ± 0.194[e]	0.593 ± 0.01[f]

Data are medium ± MSE of four independent analyses. Different superscript letters in the same column depict significant results in accordance with one-way ANOVA and Tukey's *post hoc* test ($p < 0.05$).

Considering the numerous procyanidin derivatives that were detected in the analysis of flavonoids, phenolic acids and tannins shown in Table 2, it seems reasonable to hypothesize that several of them might have contributed to the inhibitory effects on the α-amylase.

The varying strengths of interaction with the α-amylase can be partially attributed to distinct molecular structures, leading to differences in chemical binding with amino acid residues at the active site. The optimal poses of each molecule within the active site were determined, and their interactions with the enzyme are illustrated at the top of Fig. 9. The lower part of this figure exhibits interactions between inhibitor molecules and H-bond acceptor and donor atoms in the active site. Procyanidin B2 is a compound bearing several hydroxyl groups and it engages in four hydrogen bonds with residues Gln78A, Thr178A, His116A, and His320A. Masoprocol within the active site was surrounded by side chain residues such as Asp212A, Glu248A, and Asp315A by means of hydrogen binding, and Tyr77A and Trp 74A very probably by hydrophobic and van der Waals interactions. Chenodeoxycholic acid is a steroid that exhibits three polar groups, but only one establishes an H-bond with Glu248A in the active site and hydrophobic contacts with the residues Leu177A and Ile250A. Both ursodiol and lenticin exhibit a big hydrophobic area as well as polar groups that can make hydrophobic interactions and H-bonds with the active site (structure illustrated in the ESI†). It has been demonstrated that the amino acids on the active site of pancreatic α-amylase form hydrogen bonds with ligand hydroxyl groups, as well as other interactions such as hydrophobic interactions and Pi–Pi interactions. These interactions contribute to a favorable docking score.[46,47]

Table 4 also displays the six molecules present in the seed extract that were best docked into the active site of the lipase. All these compounds showed a stronger interaction with amino acid residues at the active site compared to the crystallized enzyme with methoxyundecylphosphinic acid and also with the enzyme docked with orlistat, a reference enzymatic inhibitor used *in vivo* assays. Orlistat is an FDA approved drug for obesity treatment. Several studies have shown, however, that orlistat treatment carries a potential risk of renal failure, oily stools, diarrhea, cholelithiasis, and subacute liver failure.[63] The best inhibitor, as indicated by the MRS, was ursodiol, followed by masoprocol, chenodeoxycholic acid, procyanidin B2, 13-keto-9*Z*,11*E*-octadecadienoic acid and ceratodictyol. All of these exhibited a higher probability of anchoring to the active site compared to orlistat and can therefore be considered potential candidates for exploration as naturally occurring pancreatic lipase inhibitors. Except procyanidin B2, all the other compounds were only found in the seed extract. Fig. 10 shows that the active site of the lipase is surrounded by hydrophobic as well as polar amino acids. The latter areas are shown by colored markings. The interactions consist of at least three hydrogen bonds (77B, Asp79B and Ala259B) and an ample area of hydrophobic and van der Waals interactions. The intermolecular interaction pictures, visualizing and matching both the top and bottom pictures of Fig. 10, allow us

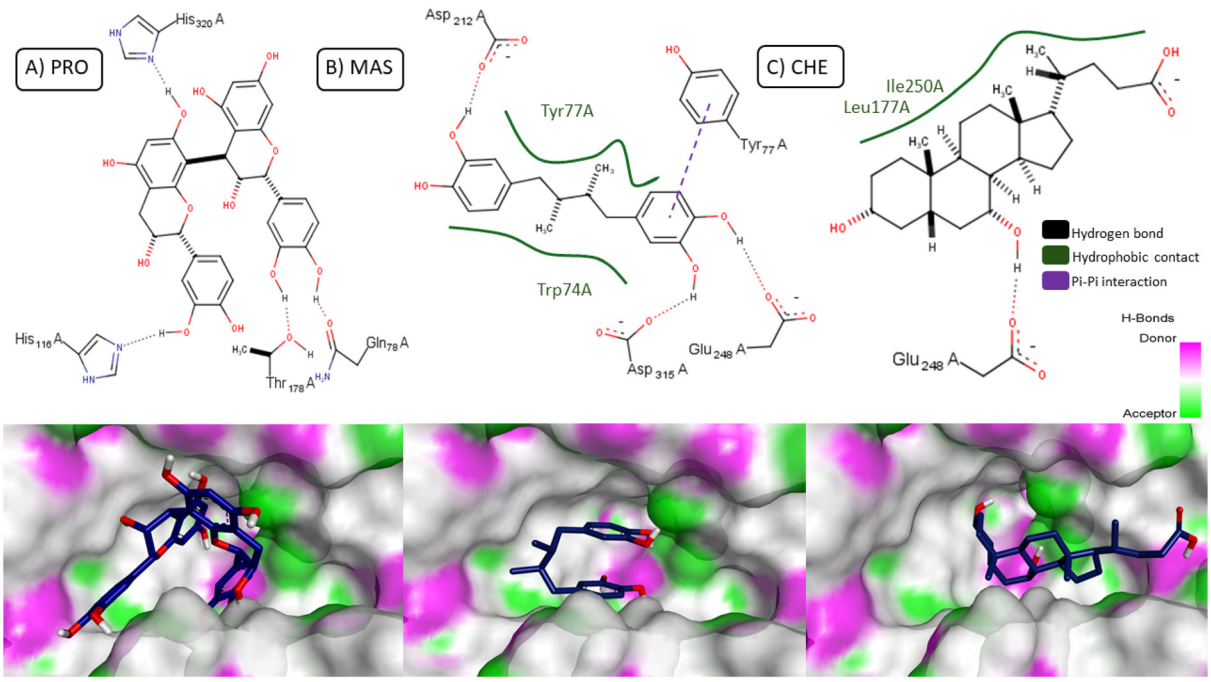

Fig. 9 Chemical structures of three best inhibitors bond (on the top) and docking interaction (on the bottom) at the active site of α-amylase. 2D interaction diagrams were generated by using the PoseView server. Poses were found by using AutoDock Vina as described in the Materials and methods section. A detailed close-up of the binding interaction with the protein structure represented in a surface model and the ligand in a stick model was generated using Discovery Studio 2021. PRO: procyanidin B2; MAS: masoprocol; and CHE: chenodeoxycholic acid.

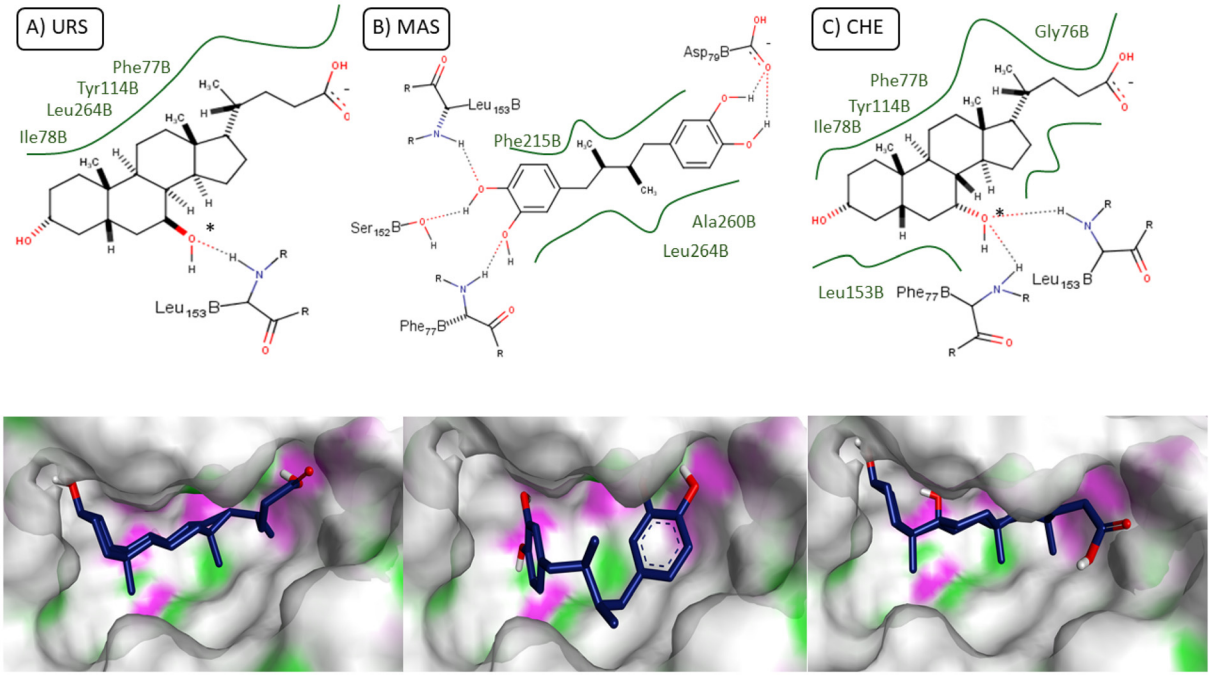

Fig. 10 Chemical structures of the three best inhibitors bond (on the top) and docking interaction (on the bottom) at the active site of pancreatic lipase. 2D interaction diagrams were generated by using the PoseView server. Poses were found by using AutoDock 4.2.3 as described in the Materials and methods section. A detailed close-up of the binding interaction with the protein structure represented in a surface model and the ligand in a stick model was generated using Discovery Studio 2021. URS: ursodiol; MAS: masoprocol; and CHE: chenodeoxycholic acid.

to show how important are the reactive residues at the active site of lipase, identifying areas that are able to form hydrogen bonds.

It is important to note that docking scores should not be interpreted as binding affinities, since the latter can only be estimated by calculations and confirmed by binding kinetic assays with the enzyme. The docking simulation only selects the molecule with physicochemical requirements needed to fit in a particular site of the protein. However, if different programs find the same pose for a given molecule in all simulations, there are great chances of it being a true ligand. Therefore, considering the docking simulations with both α-amylase and lipase, it can at least be hypothesized that the various compounds that were solely found in the seed extract can be considered as potential contributors to the inhibition of these enzymes. The molecular docking results provide significant insights into the therapeutic potential of tamarind-derived bioactives. Several tamarind-derived compounds demonstrated to possess binding affinities comparable to, or exceeding, those of existing pharmaceuticals such as acarbose and orlistat. This means that tamarind-derived compounds exhibit promising potential for the dual inhibition of α-amylase and lipase, effectively addressing hyperglycemia and obesity in a synergistic manner. Unlike many pharmaceuticals that target a single pathway, these compounds offer a multifaceted approach, enhancing their therapeutic value. Additionally, tamarind by-products are both inexpensive and widely available, making them a cost-effective and accessible alternative to synthetic drugs. Their integration into functional foods or nutraceutical formulations could provide an innovative, non-pharmaceutical strategy for the prevention and management of metabolic disorders, particularly in resource-constrained settings. Further rigorous preclinical and clinical studies are crucial to effectively translate these findings into practical clinical applications. A definitive proof in this respect can only be produced after quantification of these compounds in the seed and isolation followed by actual measurements of their inhibitory activity.

4. Conclusion

The main question that was formulated in this study was if extracts of various *T. indica* wastes, prepared under the same conditions, can eventually act as similar or different inhibitors of the pancreatic α-amylase and lipase and, consequently, act as starch and triglyceride absorption inhibitors in an animal model. In this regard, a general affirmative response was obtained, the seeds turning out as the most promising tamarind waste. The tamarind hydroalcoholic seed extract revealed to be the by far best inhibitor of α-amylase and consequently also the best inhibitor of starch absorption in mice. Furthermore, the seed extract was the only one that inhibited the pancreatic lipase and, in consequence, triglyceride absorption. The latter occurred to a degree similar to starch absorption inhibition. Furthermore, attempts at characterizing the

distinct extracts and identifying the molecules of the seed extract that could be responsible for the effects were also undertaken. In this respect, however, the data merely allowed hypotheses about the compounds that are more likely involved. Most probably the effects result from a summation of the actions of various compounds. Interestingly, however, the seed extract revealed to possess several compounds that were not found in the other extracts and which, as indicated by computer simulations, might be active as inhibitors of both α-amylase and lipase. The tamarind seed extract, which can be considered a by-product of the tamarind agricultural and industrial sector, was by far the most promising inhibitor of both starch and triglyceride digestion. These actions can be regarded as parts of a set of events that can eventually translate into weight loss, depending on the quantity and regularity of ingestion. It is worth highlighting that the extracts prepared from agro-industrial wastes are of low cost and that they present a way for reintegrating them into the productive chain. Further studies are evidently necessary for assessing safety and optimizing doses and, perhaps, for identifying the compounds that are responsible for the effects.

Abbreviations

IC_{50} Sample concentration, providing 50% of maximum antioxidant activity
ID_{50} Sample dose, providing 50% of maximum antioxidant activity
k_{frap} Rate constant

Author contributions

Adelar Bracht: data curation, funding acquisition, formal analysis, and writing – review and editing. Anacharis B. Sá-Nakanishi: conceptualization, writing – original draft, data curation, project administration and supervision. Beatriz P. Silva: investigation and data curation. Eduardo J. Pilau, investigation and data curation. Felipe de O. Souza: investigation. Gabriel A. V. Neto: investigation and data curation. Gustavo H. Souza: investigation and data curation. Jurandir F. Comar: methodology and validation. Lillian Barros: investigation, visualization and data curation. Lívia Bracht: methodology and supervision. Paulo S. A. Bueno: investigation. Rosane M. Peralta: writing – review, funding acquisition and resources. Thalita F. D. Santos: investigation. Tiane C. Finimundy: investigation.

Ethical approval

The current study is approved by the State University of Maringá (UEM) institutional ethics committee (license no. 9905181121) and the experiments were conducted following the international standards and ethical guidelines on animal welfare.

Data availability

The data supporting this article have been included as part of the ESI.†

Conflicts of interest

The authors declare no conflicts of interest.

Acknowledgements

This study was financially supported by a grant from the Council for Scientific and Technological Development (CNPq; 304090/2016-6), and the Araucaria Foundation (FA160/2022), Brazil. The authors are grateful to the Council for Scientific and Technological Development (CNPq), the Araucaria Foundation (FA), the Coordination for the Improvement of Higher Education Personnel (CAPES), the Complex of Research Support Centers of the State University of Maringá (COMCAP-UEM), the State University of Maringá (UEM), the Foundation for Science and Technology (FCT, Portugal) for financial support from the FCT/MCTES (PIDDAC) national funds to CIMO (UIDB/00690/2020 (**https://doi.org/10.54499/UIDB/00690/2020**) and UIDP/00690/2020 (**https://doi.org/10.54499/UIDP/00690/2020**)) and SusTEC (LA/P/0007/2020 (**https://doi.org/10.54499/LA/P0007/2020**)), and for the individual scientific employment program contract for the L. Barros contract (CEEC-INST, **https://doi.org/10.54499/CEECINST/00107/2021/CP2793/CT0002**).

References

1 WHO, World Health Organization, *Health topics – Obesity*, 2021. < **https://www.who.int/health-topics/obesity**>. Accessed in January, 2022.
2 I. Funke and M. F. Melzing, Traditionally used plants in diabetes therapy – phytotherapeutics as inhibitors of α-amylase activity, *Rev. Bras. Farmacogn.*, 2006, **16**, 1–5, DOI: **10.1590/S0102-695X2006000100002**.
3 B. Mayur, S. Sandesh, S. Shruti and S. Sung-Yum, Antioxidant and α-glucosidase inhibitory properties of Carpesium abrotanoides L., *J. Med. Plants Res.*, 2010, **4**(15), 1547–1553, DOI: **10.5897/JMPR10.210**.
4 M. H. Yang, Y. W. Chin, K. D. Yoon and J. Kim, Phenolic compounds with pancreatic lipase inhibitory activity from Korean yam (*Dioscorea opposita*), *J. Enzyme Inhib. Med. Chem.*, 2014, **29**, 1–6, DOI: **10.3109/14756366.2012.742517**.
5 J. Kang and C. Park, Anti-obesity drugs: a review about their effects and safety, *Diabetes Metab. J.*, 2012, **36**, 13–25, DOI: **10.4093/dmj.2012.36.1.13**.
6 H. Wang, C. Wang, Y. Zou, J. Hu, Y. Li and Y. Cheng, Natural polyphenols in drug delivery systems: Current status and future challenges, *Giant*, 2020, **3**, 100022, DOI: **10.1016/j.giant.2020.100022**.

7 S. Azad, Tamarindo—Tamarindus indica, in *Exotic fruits*, Academic Press, 2008, vol. 1, pp. 403–412. DOI: 10.1016/B978-0-12-803138-4.00055-1.
8 R. S. Glew, D. J. Vanderjagt, L. T. Chuang, Y. S. Huang, M. Milson and R. H. Glew, Nutrient content of four edible wild plants from West Africa, *Plant Foods Hum. Nutr.*, 2005, **60**, 187–193, DOI: 10.1007/s11130-005-8616-0K.
9 K. El-Siddig, H. P. M. Gunasena, B. A. Prasad, D. K. N. P. Pushpakumara, K. V. R. Ramana, P. Vijayanand and J. T. Williams, *Southampton Centre for Underutilised Crops*, Feedipedia, Southampton, UK, 2006. Accessed August 9, 2024. [https://www.feedipedia.org/node/4264].
10 T. Nofianti, S. Nurmayasari, M. Priatna, R. Ruswanto and M. Nurfatwa, The effect of the ethanolic extract of Asam Jawa leaf (*Tamarindus Indica* L.) in total cholesterol, triglyceride, LDL and HDL concentration on male Sprague-Dawley rats, *J. Phys.: Conf. Ser.*, 2019, **1179**(1), 012175, DOI: 10.1088/1742-6596/1179/1/012175.
11 N. Koyagura, H. Kumar, M. G. Jamadar, S. V. Huigol, N. I. M. Nayak, S. Yendigeri and M. Shamsuddin, Antidiabetic and hepatoprotective activities of *Tamarindus indica* fruit pulp in alloxan-induced diabetic rats, *Int. J. Pharmacol. Clin. Sci.*, 2013, **2**(2), 52029688.
12 K. F. Azman, Z. Amom, A. Azlan, N. M. Esa, E. M. Ali, Z. M. Shah and K. K. A. Kadir, Antiobesity effect of *Tamarindus indica* L. pulp aqueous extract in high-fat diet-induced obese rats, *J. Nat. Med.*, 2012, **66**, 333–342, DOI: 10.1007/s11418-011-0597-8.
13 V. Jindal, D. Dhingra, S. Sharma, M. Parle and R. K. Harna, Hypolipidemic and weight-reducing activity of the ethanolic extract of *Tamarindus indica* fruit pulp in cafeteria diet- and sulpiride-induced obese rats, *J. Pharmacol. Pharmacother.*, 2011, **2**(2), 80–84, DOI: 10.4103/0976-500X.81896.
14 F. Martinello, S. M. Soares, J. J. Franco, A. C. Santos, A. Sugohara, S. B. Garcia, C. Curti and S. A. Uyemura, Hypolipemic and antioxidant activities from *Tamarindus indica* L. pulp fruit extract in hypercholesterolemic hamsters, *Food Chem. Toxicol.*, 2006, **44**(6), 810–818, DOI: 10.1016/j.fct.2005.10.011.
15 A. N. Ukwuani-Kwaja, M. G. Abukakar and R. A. Shehu, Antiobesity effects of pulp extract *Tamarindus indica* in albino rat, *Asian J. Biochem.*, 2008, **3**(4), 221–227, DOI: 10.5555/20083213106.
16 U. E. Uchenna, A. B. Shori and A. S. Baba, An in vivo study on the effects of *Tamarindus indica* seeds in improving carbohydrate and lipid metabolism, *J. Ayurveda Integr. Med.*, 2018, **9**(4), 258–265, DOI: 10.1016/j.jaim.2017.06.004.
17 R. Maiti, U. K. Das and D. Ghosh, Attenuation of hyperglycemia and hyperlipidemia in streptozotocin-induced diabetic rats by aqueous extract of seed of *Tamarindus indica*, *Biol. Pharm. Bull.*, 2005, **28**(7), 1172–1176, DOI: 10.1248/bpb.28.1172.
18 M. Yerima, J. A. Anuka, O. A. Salawu, I. Abdu-Aguye and Y. Tanko, Antihyperglycaemic activity of the flavonoid-rich fraction of the extract of *Tamarindus indica* L. on experimentally induced hyperglycaemic wistar rats, *J. Appl. Pharm. Sci.*, 2014, **4**(8), 064–068, DOI: 10.7324/JAPS.2014.40813.
19 C. A. Aprilia, G. Ninditasari and D. Walujo, Hypolipidemic effect and antioxidant activity of Tamarind leaves extract in hypercholesterol-fed rats, *Indonesian J. Cardiol.*, 2017, **38**, 72–80, DOI: 10.30701/ijc.v38i2.730.
20 S. S. Sole, B. P. Srinivasan and A. S. Akarte, Anti-inflammatory action of tamarind seeds reduces hyperglycemic excursion by repressing pancreatic β-cell damage and normalizing SREBP-1c concentration, *Pharm. Biol.*, 2013, **51**(3), 350–360, DOI: 10.3109/13880209.2012.729067.
21 T. Buchholz and M. F. Melzig, Medicinal plants traditionally used for treatment of obesity and diabetes mellitus–screening for pancreatic lipase and α-Amylase inhibition, *Phytother. Res.*, 2016, **30**(2), 260–266, DOI: 10.1002/ptr.5525.
22 M. A. Bhutkar and S. B. Bhise, In vitro assay of alpha amylase inhibitory activity of some indigenous plants, *Int. J. Chem. Sci.*, 2012, **10**(1), 457–462. ISSN 0972-768X.
23 A. Parvin, M. Alam, A. Haque, A. Bhowmik, L. Ali and B. Rokeya, Study of the hypoglycemic effect of Tamarindus indica Linn. seeds on non-diabetic and diabetic model rats, *Br. J. Pharm. Res.*, 2013, **3**(4), 1094–1105, DOI: 10.9734/BJPR/2013/4865.
24 P. Halagali, A. Inamdar, J. Singh, *et al.*, Phytochemicals, Herbal Extracts, and Dietary Supplements for Metabolic Disease Management, *Endocr., Metab. Immune Disord.:Drug Targets*, 2024, DOI: 10.2174/0118715303287911240409055710.
25 V. G. Correa, G. A. Gonçalves, A. B. Sá-Nakanishi, I. C. F. R. Ferreira, L. Barros, M. I. Dias, E. A. Kehnlein, C. G. M. de Souza, A. Bracht and R. M. Peralta, Effects of in vitro digestion and in vitro colonic fermentation on stability and functional properties of yerba mate (Ilex paraguariensis A. St. Hil.) beverages, *Food Chem.*, 2017, **237**, 453–460, DOI: 10.1016/j.foodchem.2017.05.125.
26 L. S. Castro, L. Bracht, R. M. Peralta, H. V. Pereira-Maróstica, J. F. Comar and A. B. Sá-Nakanishi, Free radical quenching in liver mitochondria by selected antioxidants abundant in foods and supplements, *Food Biosci.*, 2023, **54**, 102925, DOI: 10.1016/j.fbio.2023.102926.
27 V. L. Singleton and J. A. Rossi, Colorimetry of total phenolics with phosphomolybdic-phosphotungstic acid reagents, *Am. J. Enol. Vitic.*, 1965, **16**(3), 144–158, DOI: 10.5344/ajev.1965.16.3.144.
28 C. G. Kato, G. A. Gonçalves, R. A. Peralta, F. A. V. Seixas, A. B. Sá-Nakanishi, L. Bracht, J. F. Comar, A. Bracht and R. M. Peralta, Inhibition of α-amylases by condensed and hydrolysable tannins: Focus on kinetics and hypoglycemic actions, *Enzyme Res.*, 2017, **2017**, 5724902, DOI: 10.1155/2017/5724902.
29 C. G. Kato-Schwartz, R. C. G. Corrêa, D. S. Lima, A. B. Sá-Nakanishi, G. A. Gonçalves, F. A. V. Seixas, C. W. I. Haminiuk, L. Barros, I. C. F. R. Ferreira, A. Bracht and R. M. Peralta, Potential antidiabetic properties of Merlot grape pomace extract: An in vitro, in silico, and

in vivo study of α-amylase and α-glucosidase inhibition, *Food Res. Int.*, 2020, **137**, 109462, DOI: 10.1016/j.foodres.2020.109462.

30 G. L. Miller, Use of dinitrosalicylic acid reagent for determination of reducing sugar, *Anal. Chem.*, 1959, **31**(3), 426–428, DOI: 10.1021/ac60147a030.

31 P. A. Castilho, L. Bracht, L. Barros, B. R. Albuquerque, M. I. Dias, I. C. F. R. Ferreira, J. F. Comar, T. B. V. da Silva, R. M. Peralta, A. B. Sá-Nakanishi and A. Bracht, Effects of a Myrciaria jaboticaba peel extract on starch and triglyceride absorption and the role of cyanidin-3-O-glucoside, *Food Funct.*, 2021, **12**(6), 2644–2659, DOI: 10.1039/D0FO02927K.

32 R. Oliveira, G. A. Gonçalves, F. D. Inácio, E. A. Koehnlein, C. G. M. de Souza, A. Bracht and R. M. Peralta, Inhibition of pancreatic lipase and triacylglycerol intestinal absorption by a pinhão coat (Araucaria angustifolia) extract rich in condensed tannin, *Nutrients*, 2015, **7**(7), 5601–5614, DOI: 10.3390/nu7075242.

33 S. M. F. Bessada, J. C. M. Barreira, L. Brasso, I. C. F. R. Ferreira and M. B. P. P. Oliveira, Phenolic profile and antioxidant activity of Coleostephus myconis (L.) Rchb. f.: An underexploited and highly disseminated species, *Ind. Crops Prod.*, 2016, **89**, 45–51, DOI: 10.1016/j.indcrop.2016.04.065.

34 P. Shannon, A. Markiel, O. Ozier, N. S. Baliga, J. T. Wang, D. Ramage, N. Amin, B. Schwikowski and T. Ideker, Cytoscape: A software environment for integrated models of biomolecular interaction networks, *Genome Res.*, 2003, **13**(11), 2498–2504, DOI: 10.1101/gr.1239303.

35 L. W. Sumner, A. Amberg, D. Barrett, M. H. Beale, R. Beger, C. A. Daykin, T. W. M. Fan, O. Fiehn, R. Goodacre, J. L. Griffin, T. Hankemeier, N. Hardy, J. Harnly, R. Higashi, J. Kopka, A. N. Lane, J. C. Lindon, P. Marriorr, A. W. Nicholls, M. D. Reily, J. J. Thaden and M. R. Viant, Proposed minimum reporting standards for chemical analysis chemical analysis working group (CAWG) metabolomics standards initiative (MSI), *Metabolomics*, 2007, **3**(3), 211–221, DOI: 10.1007/s11306-007-0082-2.

36 N. M. O'Boyle, M. Banck, C. A. James, C. Morley, T. Vandermeersch and G. R. Hutchison, Open Babel: An open chemical toolbox, *J. Cheminf.*, 2011, **3**(1), 33, DOI: 10.1186/1758-2946-3-33.

37 C. Li, A. Begum, S. Numao, K. H. Park, S. G. Withers and G. D. Brayer, Acarbose rearrangement mechanism implied by the kinetic and structural analysis of human pancreatic alpha-amylase in complex with analogues and their elongated counterparts, *Biochemistry*, 2005, **44**(9), 3347–3357, DOI: 10.1021/bi048334e.

38 M. P. Egloff, F. Marguet, G. Buono, R. Verger, C. Cambillau and H. van Tilbeurgh, The 2.46 A resolution structure of the pancreatic lipase-colipase complex inhibited by a C11 alkyl phosphonate, *Biochemistry*, 1995, **34**(9), 2751–2762, DOI: 10.1021/bi00009a003.

39 K. Gopalakrishnan, G. Sowmiya, S. S. Sheik and K. Sekar, Ramachandran plot on the web (2.0), *Protein Pept. Lett.*, 2007, **14**, 669–671, DOI: 10.2174/092986607781483912.

40 J. C. Phillips, R. Braun, W. Wang, J. Gumbart, E. Tajkhorshid, E. Villa, C. Chipot, R. D. Skeel, L. Kalé and K. Schulten, Scalable molecular dynamics with NAMD, *J. Comput. Chem.*, 2005, **26**(16), 1781–1802, DOI: 10.1002/jcc.20289.

41 W. Humphrey, A. Dalke and K. Schulten, VMD: visual molecular dynamics, *J. Mol. Graphics*, 1996, **14**(1), 33–28, DOI: 10.1016/0263-7855(96)00018-5.

42 O. Trott and A. J. Olson, AutoDock Vina: Improving the speed and accuracy of docking with a new scoring function, efficient optimization, and multithreading, *J. Comput. Chem.*, 2010, **31**(2), 455–461, DOI: 10.1002/jcc.21334.

43 G. M. Morris, R. Huey, W. Lindstorm, M. F. Sanner, R. K. Belew, D. S. Goodsell and A. J. Olson, AutoDock4 and AutoDockTools4: Automated docking with selective receptor flexibility, *J. Comput. Chem.*, 2009, **30**, 2785–2791, DOI: 10.1002/jcc.21256.

44 S. Dallakyan and A. J. Olson, Small-molecule library screening by docking with PyRx, *Methods Mol. Biol.*, 2015, **1263**, 243–250, DOI: 10.1007/978-1-4939-2269-7_19.

45 G. Jones, P. Willett, R. C. Glen, A. R. Leach and R. Taylor, Development and validation of a genetic algorithm for flexible docking, *J. Mol. Biol.*, 1997, **267**(3), 727–748, DOI: 10.1006/jmbi.1996.0897.

46 P. S. A. Bueno, C. G. Kato-Schwartz, D. S. Lima, A. Bracht, R. M. Peralta and F. A. V. Seixas, In silico evaluation of condensed and hydrolysable tannins as inhibitors of pancreatic α-amylase, *J. Mol. Model.*, 2019, **25**(9), 275, DOI: 10.1007/s00894-019-4176-3.

47 T. B. V. Da Silva, P. A. Castilho, A. B. Sá-Nakanishi, F. A. V. Seixas, M. I. Dias, L. Barros, I. C. F. R. Ferreira, A. Bracht and R. M. Peralta, The inhibitory action of purple tea on in vivo starch digestion compared to other *Camellia sinensis* teas, *Food Res. Int.*, 2021, **150**, 110781, DOI: 10.1016/j.foodres.2021.110781.

48 H. Akaike, A new look at the statistical model identification, *IEEE Trans. Autom. Control*, 1974, **19**(6), 716–723, DOI: 10.1109/TAC.1974.1100705.

49 S. Chandra, S. Khan, B. Avula, H. Lata, M.;H. Yang, M. A. Elsohly and I. A. Khan, Assessment of total phenolic and flavonoid content, antioxidant properties, and yield of aeroponically and conventionally grown leafy vegetables and fruit crops: A comparative study, *Evidence-Based Complementary Altern. Med.*, 2014, **2014**, 1–9, DOI: 10.1155/2014/253875.

50 K. P. Bastola, Y. N. Guaragain, V. Bhadriraju and P. V. Vadlani, Evaluation of standards and interfering compounds in the determination of phenolics by Folin-Ciocalteu assay method for effective bioprocessing of biomass, *Am. J. Anal. Chem.*, 2017, **8**(6), 416–431, DOI: 10.4236/ajac.2017.86032.

51 B. R. Tonsic, V. G. Correa, J. A. A. Garcia-Manieri, A. Bracht and R. M. Peralta, An in vivo approach to the reported effects of phenolic acids and flavonoids on pancreatic α-amylase activity, *Food Biosci.*, 2023, **51**, 102357, DOI: 10.1016/j.fbio.2023.102357.

52 K. Thorsen, T. Drengstig and P. Ruoff, Transepithelial glucose transport and Na^+/K^+ homeostasis in enterocytes: An integrative model, *Am. J. Physiol.: Cell Physiol.*, 2014, **307**(4), C320–C337, DOI: **10.1152/ajpcell.00068.2013**.

53 S. Reagan-Shaw, M. Nihal and N. Ahmad, Dose translation from animal to human studies revisited, *FASEB J.*, 2008, **22**(3), 659–661, DOI: **10.1096/fj.07-9574LSF**.

54 C. G. Kato-Schwarz, F. Bracht, G. A. Gonçalves, A. A. Soares, T. F. Vieira, T. Brugnari, A. Bracht and R. M. Peralta, Inhibition of α-amylases by pentagalloyl glucose: Kinetics, molecular dynamics and consequences for starch absorption, *J. Funct. Foods*, 2018, **44**, 265–273, DOI: **10.1016/j.jff.2018.03.025**.

55 Y. Sawada, R. Nakabayashi, Y. Yamada, M. Suzuki, M. Sato, A. Sakata, K. Akiyama, T. Sakurai, F. Matsuda, T. Aoki, M. Y. Hirai and K. Saito, RIKEN tandem mass spectral database (ReSpect) for phytochemicals: A plant-specific MS/MS-based data resource and database, *Phytochemistry*, 2012, **82**, 38–45, DOI: **10.1016/j.phytochem.2012.07.007**.

56 I. J. Forsythe and D. S. Wishart, Exploring human metabolites using the human metabolome database, *Curr. Protoc. Bioinf.*, 2009, **25**(1), 14.8.1–14.8.45, DOI: **10.1002/0471250953.bi1408s25**.

57 H. Horai, M. Arita, S. Kanaya, Y. Nihei, T. Ikeda, K. Suwa and T. Nishioka, MassBank: a public repository for sharing mass spectral data for life sciences, *J. Mass Spectrom.*, 2010, **45**(7), 703–714, DOI: **10.1002/jms.1777**.

58 L. Guangxiang, T. Fangfang, Y. Zhenzhen, L. Gang, H. Jie, W. Zhenhua and W. Honglun, Hypaphorine, an Indole Alkaloid Isolated from Caragana korshinskii Kom., Inhibits 3T3-L1 Adipocyte Differentiation and Improves Insulin Sensitivity in Vitro, *Chem. Biodiversity*, 2017, **14**(7), e1700038, DOI: **10.1002/cbdv.201700038**.

59 G. Cong, L. Ya, M. Fan, L. Yajie, M. Qin, L. Shu and T. Haoru, Nordihydroguaiaretic acid treatment on the antioxidant properties of strawberry fruit, *AIP Conf. Proc.*, 2018, **1956**(1), 020024, DOI: **10.1063/1.5034276**.

60 V. Desseaux, P. Socker, P. Brouant and E. H. Ajandouz, The mechanisms of alpha-amylase inhibition by flavan-3-ols and the possible impacts of drinking green tea on starch digestion, *J. Food Sci.*, 2018, **83**(11), 2858–2865, DOI: **10.1111/1750-3841.14353**.

61 E. N. Moreno-Córdova, A. A. Arvizu-Flores, E. M. Valezuela-Soto, K. D. García-Orozco, A. Wall-Medrano, E. Alvarez-Parrilla, J. F. Ayala-Zavala, J. A. Domínguez-Avila and G. A. González-Aguilar, Gallotannins are uncompetitive inhibitors of pancreatic lipase activity, *Biophys. Chem.*, 2020, **264**, 106409, DOI: **10.1016/j.bpc.2020.106409**.

62 L. J. Usjak, V. M. Milutinovic, M. J. D. Crnogorac, T. P. Stanokkovic, M. S. Niketic, J. M. Kukic-Markovic and S. D. Petrovic, Barks of Three Wild Pyrus Taxa: Phenolic Constituents, Antioxidant Activity, and in Vitro and in Silico Investigations of α-Amylase and α-Glucosidase Inhibition, *Chem. Biodivers.*, 2021, **18**(10), 2100446, DOI: **10.1002/cbdv.202100446**.

63 B. Buysschaert, S. Aydin, J. Morelle, M. P. Hermans, M. Jadoul and N. Demoulin, Weight loss at a high cost: Orlistat-induced late-onset severe kidney disease, *Diabetes Metab.*, 2016, **42**(1), 62–64, DOI: **10.1016/j.diabet.2015.08.006**.